Materials Research. 2022; 25:e20210540
DOI: https://doi.org/10.1590/1980-5373-MR-2021-0540

An Overview of the Interactions Between Reinforcements and Al Matrices with Si, Cu And Mg as Alloying Elements in Aluminum Matrix Composites: Case of Oxide Reinforcements

C.T. Guerrero**[a]**, F. González**[b]**, T.E. Soto**[a]**, C. Aguilar**[c]**, I.A. Figueroa**[d]**,
G. González**[d]**, J. Vargas**[a]**, I. Alfonso**[a,b]***

[a]Universidad Nacional Autónoma de México, Instituto de Investigaciones en Materiales, Unidad Morelia, Campus Morelia UNAM, Antigua Carretera a Pátzcuaro No. 8701, Col. Ex-Hacienda de San José de la Huerta, 58190, Morelia, Michoacán. México.
[b]Universidad Autónoma Metropolitana-Iztapalapa, Departamento de Ingeniería de Procesos e Hidráulica, 55-534, 09340, Ciudad de México, México.
[c]Universidad Técnica Federico Santa María, Department of Metallurgical and Materials Engineering, Av. España 1680, Casilla 110-V, Valparaíso, Chile.
[d]Universidad Nacional Autónoma de México, Instituto de Investigaciones en Materiales, Circuito Exterior S/N, Cd. Universitaria, 04510, Ciudad de México, México.

Received: October 18, 2021; Accepted: October 30, 2021

Oxides (Al_2O_3, SiO_2, TiO_2, ZrO_2, Y_2O_3, CeO_2, MgO) are among the most used reinforcements for Aluminum Matrix Composites (AMC); while the combination of Al with Si, Cu and/or Mg excels among the alloying systems used as matrices. Some works in literature study the effects of the reinforcements and the alloying elements on the composites manufacturing, microstructure and mechanical properties. Nevertheless, it is necessary a recompilation of the interactions oxide reinforcement-alloyed matrix, including the reciprocal effects between them. Our search revealed that not only reactions occur at the interfacial regions, but also other phenomena depending on the reinforcement characteristics and the matrix composition, which affect mechanical properties. These phenomena include modifications in the matrix microstructure and its precipitation process, diffusion of elements through the interfaces, change in the reinforcement wettability by the liquid metal, loss of alloying elements, and deterioration of the reinforcement. This work presents the occurrence of these phenomena for Al matrices with different contents of Si, Cu and Mg reinforced with the most used oxides. Its novelty lies in exploring these combinations of conditions, which could serve as a benchmark study and help for a better understanding and selection of the matrix-reinforcement system.

Keywords: *Al alloys, Al-Si-Cu-Mg, reinforcement, oxide, composite, interface.*

1. Introduction

Aluminum alloys are essential for a wide variety of applications in industries such as transportation, structural, packing, electronic, food and chemical. They present a combination of properties including low density, recyclability, corrosion resistance, high specific strength, high temperature strength and good tribological behavior[1,2]. Among these alloys are those with the presence of Si, Cu and/or Mg as alloying elements. Each one of these elements contributes to the microstructures and properties of the resulting alloys, which are used for applications according to their properties. Silicon is the most used alloying element in aluminum casting alloys[1,3-6], providing abrasion resistance, decreasing density, significantly increasing castability, and slightly improving mechanical properties. Regarding Cu, its addition increases the strength and hardness of these alloys, also improving machinability by increasing matrix hardness, although reducing the corrosion resistance[7-9]. On the other hand, Mg provides important strengthening and improvement in work hardening, also imparting good corrosion resistance[1,10-14]. The addition of these alloying elements to Al can lead to the formation of micrometric second phases or nanometric precipitates, which can be respectively obtained from the solidification process, or precipitate from a solid solution due to a heat treatment. Some of them are eutectic Si, β-Mg_2Si, θ-Al_2Cu, Al_2CuMg, and quaternary Q phase ($Al_5Cu_2Mg_8Si_6$)[13-19], and in some cases they could be considered reinforcements of the alloys and part of in-situ composites (e.g. Mg_2Si and Al_2Cu[20-24]). Second phases, precipitation hardening and solid solution strengthening are among the most important hardening mechanisms for these alloys[4,7,16,25-26], which highly depend on the alloying elements content. Nevertheless, the strengthening reached by these mechanisms is not as high as desired. In search of better properties these alloys have been reinforced with particles, whiskers, fibers and nanotubes of different materials, obtaining Aluminum Matrix Composites (AMC)[27-33]. These better mechanical properties are possible by adding reinforcements with elastic moduli significantly

---

*e-mail: ialfonso@unam.mx

higher than the matrices, such as Al_2O_3 (E = 400 GPa) or SiC (E = 480 GPa). It is important to remember that the elastic modulus for an aluminum matrix is 70 GPa[1,27-33]. Elastic modulus, tensile strength, and high temperature stability of AMCs are higher than those of unreinforced alloys; while their ductility, fatigue and fracture toughness are significantly lower[27-31]. When aluminum and its alloys are combined with ceramic reinforcements intermediate properties are obtained. It is well known that metals are ductile and present low stiffness; while ceramics are stiff and with very high strength, but also are brittle and their fracture can be catastrophic. AMCs combine the great strength of the ceramics while avoiding their brittle failure, also reducing the deformation in the part of the matrix which is close to the reinforcements. The role of the aluminum matrix consists on binding and transferring load, giving its shape to the composite component; while the degree of strengthening depends on strong bonding at the matrix–particle interface[28,29,34,35]. AMC have been the most used matrix due to their lightweight and higher mechanical and thermal properties[27-29]. Al has a density of 2.7 g cm^{-3}, an elastic modulus of 70 GPa and compressive strength of ~ 450 MPa (e.g. 380 alloy)[1], while some of their most used reinforcements have similar densities (SiC 3.21 g cm^{-3}, B_4C 2.52 g cm^{-3} and Al_2O_3 3.92 g cm^{-3}) but very high elastic moduli (SiC 430 GPa, B_4C 450 GPa and Al_2O_3 350 GPa) and compressive strengths (SiC 2800 MPa, B_4C 2800 MPa and Al_2O_3 350 MPa)[36]. This wide variety of physical and mechanical properties lead to applications in industries such as transport, aeronautic, aerospace and electric, besides in a wide variety of recreational products[37]. Examples of these applications are rocker arms, brake rotors and pistons, drive shafts, core of overhead electrical conductors, energy storage flywheels, and sporting goods for golf, cycling, baseball and skiing[38,39]. Composites include Metal Matrix Syntactic Foams (MMSFs), formed by porous reinforcements or fillers[40-45], which are used in applications requiring higher mechanical properties than the obtained using conventional foams. Hollow fillers used in these materials reinforce the matrix while decreasing its density. Some of their applications are in marine equipment, sandwich parts in other composite materials, and structural components in the aerospace industry[45]. Mechanical properties of both MMC and MMSF depend on details such as the matrix composition and the reinforcement volume fraction, distribution, aspect ratio, size, orientation and interfacial bonding. For MMSF characteristics of the hollow reinforcements such as porosity percentage and wall thickness also affect the mechanical properites[45]. Among the most reported reinforcements for AMC are carbides (SiC, B_4C, WC, TiC)[46-52], oxides (Al_2O_3, SiO_2, TiO_2, ZrO_2, Y_2O_3, MgO, CeO_2)[53-58], nitrides (Si_3N_4, BN)[59-61] and Carbon Nanotubes (CNTs)[62-67]. For the case of syntactic foams there have been mainly reported metallic or ceramics hollow spheres, being Fe, SiC, SiO_2 and Al_2O_3 the most used[40-45,68-72].

Ceramic oxides represent an important part of these reinforcements, being essential the study of this particular group and their interactions with aluminum alloy matrices. Al is a very active metal, reacting with different reinforcements, fact that could be enhanced with the presence of alloying elements[73]. Due to the variety of matrices and reinforcements, the microstructural analysis of these materials is essential, including matrix-reinforcement interactions and their interfaces. Characterization techniques for this purpose include Optical Microscopy (OM), Scanning and Transmission Electron Microscopy (SEM and TEM, respectively), X-Ray Computed Micro-tomography (XCT) and X-Ray Diffraction (XRD)[74-77]. These studies grow in importance for matrices with more alloying elements, as the case of Al alloys with Si, Cu and Mg. The information in literature about the interfacial reactions for this alloy system with oxides in AMC is little and disperse. Researchers have mainly focused they works in analyzing the effect of the kind and percentage of reinforcements, with some works related to the study of the interfacial reactions, but few works including the effect of the alloying elements as a variable. It is reported that for AMC containing different alloying elements the improvement of the mechanical properties of the composite depends not only on the reinforcement but also on the matrix strengthening due to the alloying elements (solid solution and precipitation strengthening), and on the interfacial reactions and other interactions matrix-reinforcement[78]. Besides, most of the works found in literature only include binary or ternary alloys, and mainly with the most used reinforcements (i.e. SiC, Al_2O_3)[41,79]. This is accentuated by the fact that majority of the reviews deals only with aspects such as the effect of the reinforcement, its volume fraction and distribution. Then, it is necessary a compilation of the effect of these alloying elements on the matrix-reinforcement interactions. Except for the particular case of silicon in SiO_2, few works in literature include the analysis of the effect of the alloying elements on these interactions, being also considered that much of them do not have a significant effect on the reactions matrix-reinforcement. Maybe Mg is the second most studied element in these composites, reported as a wettability improver of the reinforcement by the liquid metal[80,81]. That is why in this review we tried to gather and compile information about these interactions and their effect on the mechanical properties of the composites. There are different mechanisms contributing to the composites yield strength (σ_y)[82], which include: the Al matrix strength (σ_m), which depends among other factors on the alloying elements forming second phases; the Hall-Petch strength (σ_{H-P}) due to the effect of grain boundaries in refined grains; the strengthening by solid solution (σ_{ss}), which depends on the alloying elements content; the precipitate strengthening (σ_{pp}) due to the precipitation of fine particles; and the strengthening due to the reinforcements (σ_r), directly affecting MMCs. In addition to this last mechanism, matrix-reinforcement interactions sum other mechanisms, as the load transfer (σ_{LT}); and thermal (σ_{TM}) and Elastic Modulus (σ_{EM}) mismatches[83-86]. Some of these mechanisms can be affected by the interactions produced when a reinforcement is added to a matrix, modifying for instance grain sizes, elements in solid solution, precipitates and their formation mechanisms, etc. That is why the aim of the present review is to analyze the information in literature describing the role of Al alloys with Si, Cu and Mg on the interaction mechanisms and interfaces formation in Aluminum Matrix Composites reinforced with different oxides, and their subsequent effect on the mechanical properties. This study could contribute to a better selection of reinforcements depending on the alloying elements content in the aluminum matrix.

2. Generalities of Interfaces

Among the most important interactions occurring when a reinforcement is immersed in a liquid metal is the formation of interfaces, which are critical for strengthening and stiffening the composite. Physical properties such as thermal conductivity, expansion, and dimensional stability are also directly related to the characteristics of the interface, which depend on details such as the manufacturing process, constituent phases composition, and time and temperature of contact reinforcement-matrix. Among the most used processes for manufacturing AMC are stir casting, infiltration, squeeze casting, compocasting and powder metallurgy[79,85-88]. The presence of different alloying elements could modify the interfaces obtained during these processes, affecting the mechanical properties. Such interactions highly depend on the manufacturing temperature, which are different according to the used process, being more determinant the interfacial effects for liquid-state processing due to the use of higher temperatures and the effect of wetting. In these processes temperature is commonly maintained between 700 and 900 °C, required for melting Al alloys.

Interfaces can be just a boundary, presenting a physical nature; or being a layer obtained due to chemical reactions, diffusion or other phenomena. These regions located around the reinforcements are of finite thickness and can contain new compounds, structural deviations, or structures and properties different from those of both matrix and reinforcement[89,90]. Although there should be avoided some adverse chemical reactions affecting matrix or reinforcement, such as those forming detrimental brittle reaction products[34], a high degree of strengthening is directly related to a strong matrix–reinforcement bonding. There are desired interfaces with atomic or molecular interactions to reach optima mechanical properties[89], being in several cases present only as inhomogeneities in the near-interface region, barely observed even using High Resolution TEM (HRTEM)[91]. According to Guo[92], from a phenomenological point of view interfaces can include physical bonding, chemical bonding, or mechanical keying. That is why the factors contributing to bonding should be analyzed at different levels and with different techniques.

3. Interactions Between Oxides and Al Alloys with the Presence of Si, Cu and Mg

The interaction between a reinforcement and a matrix, and the subsequent mechanical properties of the obtained AMC will depend on various factors as wetting, reactivity, bonding, etc., which at the same time are related to the manufacturing process and the chemical composition of the system. Interfacial reactions mainly occur when the reinforcements are in contact with molten Al alloys, but can be also present at lower temperatures due to diffusion or other processes contributing to solid state reactions.

Microstructural modifications are one of the most important results when a reinforcement is added to a molten alloy. This occurs due to temperature gradients between the molten matrix and the cooler reinforcements, affecting grain size and second phases morphologies. Besides, the volume of the molten metal decreases with the increase in the volumetric fraction of the reinforcement, leading to a faster solidification compared to the solidification process for unreinforced alloys. The solidification velocity for alloys mainly depends on the mold and not on the presence of reinforcements which could act as nucleation centers if are at temperatures lower than that of the molten metal[93]. Lower temperature and less latent heat during solidification could cause not only grain refinement but also higher matrix saturation with alloying elements and low wetting[94,95]. Fine grains can significantly increase the mechanical properties of the matrix due to the Hall–Petch effect contribution, mainly for sizes below 100 nm[96]. On the other hand, matrix composition could be altered by irreversible interfacial reactions involving reinforcement and matrix solutes. This region can influence mechanical properties, being a preferential location for precipitation and alloying elements segregation, with the presence of higher concentration of point defects or residual strains[91]. Even if the addition of reinforcements is to an age-hardenable alloy, precipitates nucleation and their growing kinetics may change significantly compared to the unreinforced alloy[97]. Then, besides the interfacial reactions it is also important to analyze the effect of other interactions which could significantly affect the mechanical properties of the composite. In the following subsections the effect of Si, Cu and Mg as alloying elements on the interfacial reactions and on other matrix-reinforcement interactions will be discussed for the most important oxide reinforcements used in AMC. The effect of these phenomena on the mechanical properties of the obtained composites will be also assessed.

3.1. Al_2O_3

Aluminum oxide (alumina, Al_2O_3), presented mainly as α-Al_2O_3, has high hardness and specific strength, is chemically resistant to bases and acids, can be used in applications needing high temperature resistant and has excellent tribological properties. It is used in applications requiring refractoriety and heat-resistance, and as abrasive, cutting or coating material[27,29]. It has been also reported as hollow reinforcement in metal matrix syntactic foams[68,98]. Al_2O_3 does not react with Al matrix[41,42], but it is susceptible to be attacked by alloys containing elements with oxides more stable than Al_2O_3 (e.g. Mg). This could limit the maximum allowable service temperature of the material because Al_2O_3 could be degraded, decreasing mechanical properties[91]. It has been reported the formation of MgO by a direct reaction due to the addition of Mg to Al alloys by the following reaction[99,100]:

$$3Mg_{(l)} + Al_2O_3(s) = 3MgO_{(s)} + 2Al_{(l)} \tag{1}$$

As a result of this reaction in extreme cases the alumina particles can change to MgO, as showed Pai et al.[101] for an Al-4.5Mg alloy. In order to promote wetting between aluminum and Al_2O_3, Mg has been used as external dopant adding it to the molten aluminum, e.g. an Al-2.8Mg-0.81Si alloy[102]. This advantageous use was also found adding 1% magnesium powder to a molten 6061 Al-0.85Mg-0.68Si-0.22Cu alloy reinforced with Al_2O_3 particles[95]. It is also reported that Mg reduces particles clustering[103] because it can act increasing the reinforcement surface energy, decreasing the matrix surface tension, and/or decreasing the reinforcement-matrix energy on the interface. This was corroborated by Chen et al.[104], who demonstrated that Mg- and Cu-doped interfaces presented uniform charge distribution, granting excellent tensile properties.

Janowski and Pletka[105] found the presence of a Si-rich oxide-based amorphous phase at the interface for Al-4.4Cu-0.5Mg-Si and Al-0.25Cu-1.0Mg-0.6Si alloys reinforced with 9 and 18 vol.% of Al_2O_3 particles. This was effect of the locally high Si content near Al_2O_3, and led to diminish mechanical properties due to debonding which occurred as a result of the fracture of the layer surrounding the reinforcement.

Mg enrichment of the matrix at the interface has been reported, even with appreciable magnesium penetration into the reinforcement. Munitz et al.[106] used Auger Electron Spectroscopy and Electron Diffraction for the analysis of an Al-4Mg reinforced with Al_2O_3 fibers, finding that when Al_2O_3 was added to the molten alloy the formation of the spinel phase $MgAl_2O_4$ occurred (MgO was also detected), this according to the following reaction[107-111]:

$$3Mg_{(l)} + 4Al_2O_{3(s)} = 3MgAl_2O_{4(s)} + 2Al_{(l)} \tag{2}$$

These results show that the formation of MgO or/and $MgAl_2O_4$ may occur with similar Mg contents (Pai et al.[101] obtained MgO using Al-4.5Mg/Al_2O_3 particles at 850 °C, while Munitz et al.[106] obtained both MgO and $MgAl_2O_4$ using Al-3.8Mg/Al_2O_3 fibers stirred at 685°C during 30 min). This demonstrates the importance of the manufacturing process and the control of parameters such as temperature and time of contact matrix-reinforcement. More research is needed on this topic, because in addition to the formation of Mg and $MgAl_2O_4$ through Equations 1 and 2, both compounds can be obtained following the sequence[112]:

$$Mg_{(l)} + Al_2O_{3(s)} \rightarrow \delta - MgAl_{26}O_{40(s)} \rightarrow MgAl_2O_{4(s)} \rightarrow MgO_{(s)} \tag{3}$$

$MgAl_2O_4$ has chemical inertness, high melting point, good thermal shock resistance, and high mechanical strength at elevated temperatures[113-115]. Its formation has been also reported from de melt due to the presence of oxygen as follows[109-111]:

$$Al_{(l)} + Mg_{(l)} + O_{2(g)} = MgAl_2O_{4(s)} \tag{4}$$

The formation of the spinel phase through these reactions also includes a reverse reaction, leading to its degradation:

$$MgAl_2O_{4(s)} + Mg_{(l)} = MgO_{(s)} + Al_{(l)} \tag{5}$$

The presence of Mg not always leads to the formation of these Mg-rich compounds, because it depends on the kind of alumina. For example, Bacciarini and Mathier[116] demonstrated that Mg did not react with α−γ-amorphous Al_2O_3 for an Al6061(~1wt.% of Mg)/Al_2O_3(60% vol.) composite obtained by infiltration. Contrarily to the behavior observed for composites reinforced with α−Al_2O_3, in this case Mg remained at the matrix and contributed to the composite strengthening by Mg_2Si precipitation. This inertness alumina consisted of α−Al_2O_3 which was modified into a mixed α−γ-amorphous Al_2O_3, and made the difference in the interfacial reaction. Its inertness was not explained by these authors, but it could be attributed to differences in wetting. It is reported that γ-Al_2O_3 present a defect structure, surface acidity and high surface which makes it useful in applications as adsorbent and catalyst support[117,118]. Otherwise, amorphous Al_2O_3 presents chemical, thermal and mechanical stability derived from its non-crystalline nature[117,118]. Molins et al.[119] also found the precipitation of Mg_2Si analyzing the behavior of the alloying elements at the interface of 20%$A1_2O_3$/(Al-2Mg-0.3Si) composites through element maps and concentration profiles along line-scans. They found important segregations of Mg and Si at the interfaces when SiO_2 was added as thin colloidal coating. These elements reacted to form Mg_2Si through Equation 6, hardening the matrix although Al-Mg alloys are not known for precipitation hardening:

$$2Mg_{(l)} + Si_{(l)} = Mg_2Si_{(s)} \tag{6}$$

In the case of Cu additions, Chawla[100] reported the formation of $CuAl_2O_4$, while Baik et al.[94] analyzed the reaction between Al_2O_3 and an Al-12Si-l.0Cu-l.1Mg-l.4Ni alloy reinforced with 20 vol.% of δ-alumina short fibers. They reported that infiltrating an Al_2O_3 preform previously heated at 600 °C led to the reaction between Mg and Al_2O_3 to form the spinel phase, besides reacting Al_2O_3 with Cu. This led to the formation of a reaction layer, corroborating the presence of Cu and Mg in excess on the fiber surface, degrading the strength of the composite. It is important to remark that the formation of the interlayer was not observed for infiltration at lower temperatures, when there was not enough wetting of the Al_2O_3 fibers by the molten alloy. Reactions involving Cu for this system are:

$$\left[Cu\right] + \tfrac{1}{2}\, O_{2(g)} + Al_2O_{3(s)} = CuAl_2O_{4(s)} \tag{7}$$

$$\left[Mg\right],\ \left[Cu\right] + 2\left[Al\right] + 2\, O_{2(g)} = MgAl_2O_4,\ CuAl_2O_{4(s)} \tag{8}$$

Another reported result derived from the interaction matrix-reinforcement is the modification of the precipitation process, as was observed by Ikeno et al.[120] using HRTEM for Al_2O_3 reinforcing Al-Cu-Mg alloys. These authors did not observe these modifications for Al-Mg-Si alloys. Otherwise Matsuda et al.[121] reported the decrease of age hardening for an Al-1%Mg_2Si alloy after adding 4% of alumina particles. Using electron diffraction and EDS (X-ray Energy Dispersive Spectroscopy) they found the formation of spinel $MgAl_2O_4$ at the interface Al_2O_3-matrix, but not as a thin layer but as plate shaped particles. For an Al-7Si-2.8Cu (in mass%) alloy the addition of Al_2O_3 fibers led to an increase in the age hardening response, significantly decreasing the time required to obtain peak hardness. For the same alloy with 0.4 mass% of Mg the reinforcement with Al_2O_3 led to a decrease in the peak ageing time, also decreasing the age hardening response. This result motivated a decrease in the composite strength, attributed to a lower Mg concentration in the matrix originated by the above commented reaction with Al_2O_3 to form the spinel $MgAl_2O_4$ phase (Equation 2). Besides, Cu segregation of about 2% at. on the interface between Al_2O_3 and an Al-1.4Cu alloy has been reported, analyzed by HAADF-STEM (High Angle Annular Dark Field-Scanning Transmission Electron Microscopy) and EDS[122], leading to heterogeneous nucleation of precipitates at the interfacial zone. Otherwise, Liu et al.[123] found that for higher Cu contents (5.3-6.4 wt.%) a soft interfacial layer increased the fracture toughness of the composite in the peak age condition. This interface presented precipitates different to the observed in the matrix, depleting the Cu concentration in the interface.

Figure 1a shows a SEM micrography for an Al_2O_3–Al(15Cu) matrix, where Al_2O_3 particles (light) are uniformly distributed[114]. In this image the eutectic second phase Al-Al_2Cu is also observed. Otherwise, Figure 1b shows a TEM image of the interface between Al_2O_3 and an Al-1.4Cu matrix, with a zigzag morphology and the presence of the intermetallic phase Al_2Cu precipitated at the interface (dark phase) due to Cu segregation[120]. Otherwise, Figure 1c-f shows bright and dark field TEM images and SADP (Selected Area Diffraction Pattern) of the interfacial layer obtained due to the reaction between γ-Al_2O_3 fiber and a matrix Al-7Si-2.8Cu-0.4Mg (in mass %). This reaction occurred during the manufacturing process, infiltrating an Al_2O_3 preform at 1073 K[112]. In this figure patterns correspond to aggregates of γ-Al_2O_3 particles of 10 nm (Figure 1d) constituting the reinforcement, and to the interfacial $MgAl_2O_4$ (Figure 1f) formed due to the presence of Mg (Equation 2). This reaction layer has 100-120 nm in thickness, and its formation leads to a reduction in the concentration of Mg available to form precipitates of λ′ phase ($Al_5Cu_2Mg_8Si_8$). Again, the formation of the spinel phase even at low Mg content reveals the narrow limit to obtain this phase according to the above presented reactions of Equations 1-3.

It has been also found that the grain size of the matrix considerably decreases with the increase in the percentage of Al_2O_3 particles, showing the influence of not only the alloying elements but also of the reinforcements[124]. Grain refinement increases yield strength and wear resistance, decreasing ultimate tensile strength and ductility.

Although important works were found related to matrix-reinforcement interactions for composites reinforced with Al_2O_3, they are focused to Al alloys with Mg as the main alloying element. The effect of Si and Cu additions needs more research, because the studies including these elements are few and basically deal with the formation of Cu and Si-rich precipitates.

3.2. SiO_2

Silicon dioxide (silica, SiO_2) has been selected as reinforcement due to its high hardness, melting point and availability, although the Al-SiO_2 composites have been barely used because of the high reactivity between these materials. The few studies found in literature reveal that they present high wear resistance and hardness, enabling their applications in severe thermal environments which demand greater mechanical properties, such as automotive parts[125-127]. Al reacts with SiO_2 through the following reaction[128]:

$$4Al_{(l)} + 3\,SiO_{2(s)} = 2Al_2O_{3(s)} + 3Si_{(s)} \qquad (9)$$

This reaction is even reported to occur at the interface in the solid state at temperatures as low as 440-550°C[128],

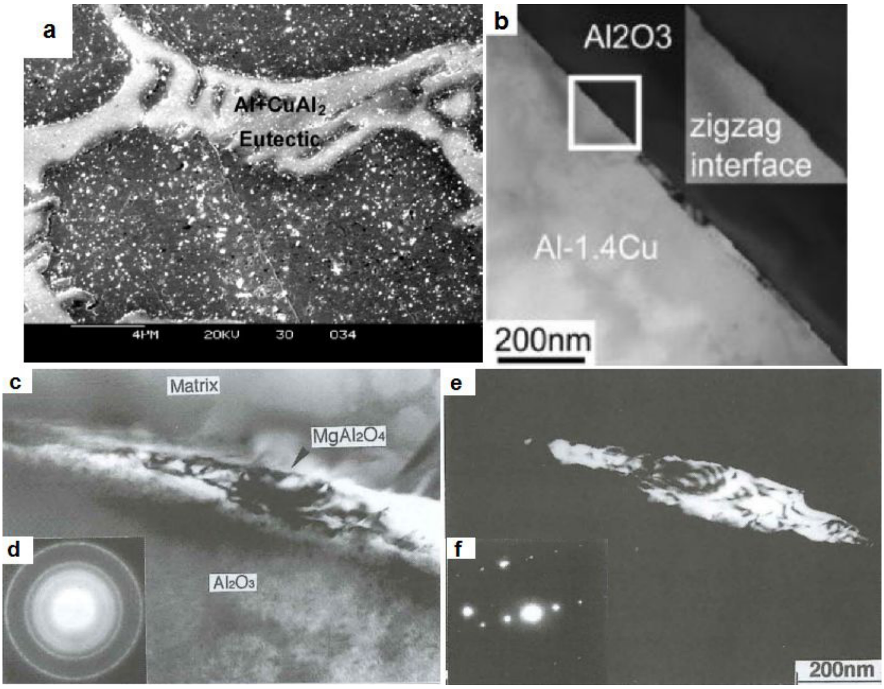

Figure 1. a) SEM image of an Al_2O_3–Al(15Cu) composite where light grey Al_2O_3 particles are observed (reproduced with permission from[114]). b) Bright field TEM micrograph for the interface Al_2O_3-matrix (Al-1.4Cu alloy) (reproduced with permission from[122]). c-f) Interface reaction layer Al_2O_3/Al-Si-Cu-Mg matrix: c) bright field TEM image, d) SADP identifying Al_2O_3, e) dark field TEM image, and f) SADP for the interface ($MgAl_2O_4$). (reproduced with permission from[112]).

and can be used for fabricating Al_2O_3 reinforced AMCs[129]. Gregolin et al.[130] found that an Al-5SiO_2 (in wt.%) fiber composite changed into another composite after being heat-treated at 600 °C. The original fibrillar morphology was retained but its composition changed from SiO_2 to Al_2O_3. Orbulov et al.[131] found that for hollow SiO_2 spheres used in syntactic foams this reaction also occurs. These authors revealed that the reaction degraded SiO_2, but did not occur for matrices with about 12 wt% of Si, where SiO_2 remained stable. Then, a possible route for manufacturing these composites without the degradation of the reinforcement could be the use of high content of this alloying element. The same behavior will be further observed for other reinforcements, where adding as alloying element the same element of the oxide minimizes or even avoids the reduction reaction. More research is necessary for stablishing in each case the correct combination of alloying elements content and processing conditions, such as temperature and time. Figure 2a-c shows[129] the kinetic model of the reaction present in Equation 9, indicating that when the temperature increases to the melting point of the aluminum alloy, solid Al melts and surrounds SiO_2, forming the interfaces Al-SiO_2 (Figure 2a). As the temperature increases the reaction continues with the formation of Al_2O_3 and solid Si at the interfaces (see Figure 2b). These new phases then leave the interfaces and diffuse into the liquid Al matrix, being obtained Si blocks and Al_2O_3 particles as final products of the reaction (Figure 2c)[129]. This is shown in Figure 2d-f for a real composite, where first Si is displaced by the reaction between SiO_2 particles and the Al matrix, surrounding the particles (Figure 2d); followed by the formation of an outer layer of Al_2O_3 (Figure 2e); and the final total transformation from SiO_2 to Al_2O_3[132]. This reaction not only leads to modify the reinforcement, but also to obtain a different matrix with the presence of Si, which could affect properties such as wear resistance and strength.

Although as it was observed in Fig. 2d-f Wang and Shi[132] did not obtain other reaction products apart from Al_2O_3 and Si, it is reported that besides Equation 9 another possible reaction occurs at solid state due to the interaction of alumina and silica, being obtained $Al_6Si_2O_{13}$ as follows[132]:

$$3Al_2O_{3(s)} + 2SiO_{2(s)} = Al_6Si_2O_{13(s)} \tag{10}$$

This reaction may be favored at low temperatures, although eventually $Al_6Si_2O_{13}$ will transform to Al_2O_3 as follows:

$$8Al_{(l)} + 3\,Al_6Si_2O_{13(s)} = 3Al_2O_{3(s)} + 6Si_{(s)} \tag{11}$$

Microsegregation of second phases in the interfaces has been reported for an Al-4Cu-1Mg-0.04Si alloy AMC reinforced with Al_2O_3, with the presence of SiO_2 as a binder in the manufacturing process. This study of Cayron[87] revealed that Mg reacted to form MgO and spinel $MgAl_2O_4$, which was determined using EDS and SAED (Small Angle Electron Diffraction) through TEM[87]. This author reported the following reactions:

$$Mg_{(l)} + 2SiO_{2(s)} + Al_{(l)} = MgAl_2O_{4(s)} + 2Si_{(s)} \tag{12}$$

$$2Mg_{(l)} + SiO_{2(s)} = 2\,MgO_{(s)} + Si_{(s)} \tag{13}$$

$$2MgAl_2O_{4(s)} + 3Si_{(l)} = 2\,MgO_{(s)} + 3SiO_{2(s)} + 4Al_{(l)} \tag{14}$$

$$3SiO_{2(s)} + 2\,MgO_{(s)} + 4Al_{(l)} = 2MgAl_2O_{4(s)} + 3Si_{(l)} \tag{15}$$

SiO_2 is found to be an important oxygen source in the formation of $MgAl_2O_4$ in Al alloys with the presence of Mg. The reactivity of SiO_2 is higher than other oxygen sources such as Al_2O_3, MgO and TiO_2[113,116]. Low Mg content favors the formation of $MgAl_2O_4$ according to the reaction in Equation 12, while high Mg content tends to form MgO according to the reaction in Equation 13[133,134]. In various works Mg content is considered to be low when it is lower than 4 at.%, favoring Equation 10[134-139] and the formation of the spinel phase. Nevertheless, Sato and Mehrabian[140] reported that the spinel $MgAl_2O4$ is obtained if the concentration of Mg in the melt is in the range 0.04-1.7 wt% Mg, while MgO

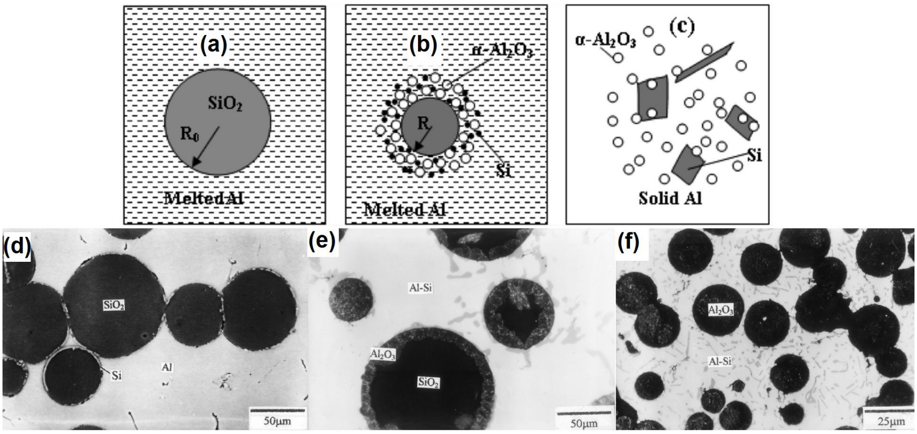

Figure 2. Models illustrating the reaction between SiO_2 and Al matrix to obtain Al_2O_3 and Si. (a) before the interfacial reaction; (b) during the reaction; (c) at the end of the interfacial reaction. (Reproduced with permission from[129]). (d-f) Microstructures for real composites at different stages of the SiO_2-Al interfacial reaction: (d) SiO_2-Al composite, where a Si layer is observed surrounding SiO_2; (e) SiO_2-AlSi composite, where the Si layer changed to Al_2O_3; and (f) Al_2O_3-AlSi composite after the final transformation from SiO_2 to Al_2O_3. (Reproduced with permission from[132]).

is obtained for concentrations higher than about 1.7 wt%. That is why special attention must be paid in order to adequately control these reactions.

In some cases, most of Mg within the matrix could be consumed as a result of the interfacial reaction with SiO_2, leading to the absence of Mg-rich precipitates, e.g. Al_2CuMg. These precipitates are responsible of the matrix strengthening, and their absence it is reported to decrease mechanical properties[134]. Besides, the bonding strength between $MgAl_2O_4$ and Al is higher than that between Al_4C_3 and Al[134,141], modifying the fracture mechanism of the particles from pull-out to tensile loading-induced fracture. Then, Mg content in the matrix needs to be controlled, being reported a substantial increase in the hardness of both the composites and the matrices by increasing the amount of Mg[134]. Mg and Si released from the interfacial reactions can combine to form Mg_2Si according to Equation 6, hardening the Al-Mg matrix in not heat treatable alloys. The original Al–Mg matrix are reported to changes to Al–Mg–Si due to the reduction of SiO_2 and consumption of Mg, precipitating Mg_2Si mainly along the grain boundaries[80,142,143].

The addition of Mg into the aluminum melt helps to improve the wettability of SiO_2 with matrix by increasing the surface energy of solid, decreasing surface tension of liquid, and decreasing the particle/alloy interfacial energy. Besides, this element increases the interface bonding strength[78,80,144].

No interfacial products are reported involving Cu, but only the precipitation of Cu-rich phases such as Al_2Cu and Al_2CuMg, according to the composition of the matrices[87, 134]. This shows that Cu presents a reactivity with this reinforcement even lower than the observed for Al_2O_3. Nevertheless, more research is needed to support this asseveration, because as was above mentioned Al-SiO_2 composites have been barely used.

3.3. TiO_2

Titanium dioxide (titanium (IV) oxide, titania, TiO_2) has high tensile strength, impact strength and hardness, being used for reinforcing AMC in automotive applications[27]. Almost all the works found in literature mention the use of this ceramic combined with other reinforcements such as SiC[145]. Otherwise, the preferred manufacturing process is powder metallurgy[146], with some articles including the TiO_2 addition using welding[147] or spray formed, as the case of Al–2Mg–TiO_2 composite studied by Chaudhury and Panigrahi[148], who found good interfacial bonding. Venugopal and Karikalan[145] used stir casting to obtain hybrid metal matrix composites AA6061-TiO_2-SiC and also reported good interfacial strength, but did not make an in depth study of the interfaces. The most important reported reaction for this system is[149-151]:

$$TiO_{2\,(s)} + Al_{(l)} \rightarrow Al_2O_{3(s)} + Ti_mO_{n(s)} + Ti_xAl_{y(s)} \qquad (16)$$

This reaction it is reported to occur by the extraction of oxygen anions from TiO_2[152]. The most commonly obtained intermetallic Ti_xAl_y phases are Ti_3Al, TiAl and $TiAl_3$; while titanium Ti_mO_n oxides include Ti_2O, TiO, Ti_2O_3 and Ti_3O_5. Saboori et al.[149] found that between 800 and 1000 °C for a 6060 Al alloy (max. 0.5Mg and 0.6Si) the final products of this reaction also were $TiAl_3$ and α-Al_2O_3, while Shin et al.[153] reported that the formation of this interfacial layer has beneficial effects on the composite strength. These authors studied the evolution of the interfacial layer and the formation of reaction products due to the reaction of Equation 16, as can be seen in the schematic representation in Figure 3a-d for the morphological variations of TiO_2, resulting in the

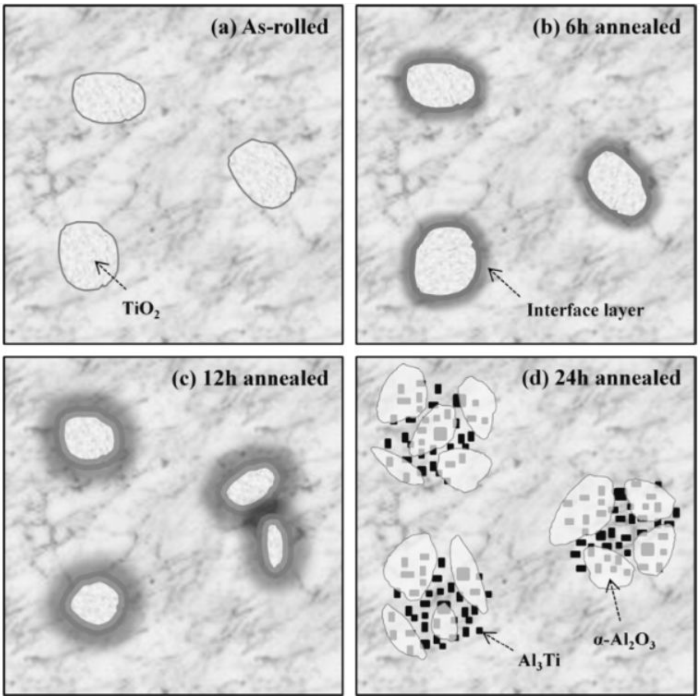

Figure 3. Schematic representation of the morphological variations of TiO_2 during annealing at 500 °C for an Al-TiO_2 composite. (a) aluminum matrix with a clearly observed interface. (b,c) O and Ti atoms decomposed from the TiO_2 diffused out to the matrix, enlarging the interfacial layer and decreasing TiO_2 size. (d) α-Al_2O_3 and Al_3Ti obtained as final reaction products. (Reproduced with permission from[153]).

formation of new reinforcements[153]. They found that this reaction can occur at temperatures as low as the annealing temperature (~ 500 °C).

Part of the above commented reaction can be observed in the TEM images of Figure 4a-d. This work of Chao et al.[154] showed that Al and TiO_2 (25% vol.) reacted during hot press sintering at 933 K, obtaining a composite Al_3Ti+Al_2O_3/Al. These authors obtained Al_3Ti of two sizes: micrometric and nanometric (~100 nm), as can be seen denoted as A and B in Figures 4a and 4b, respectively. The formation of these particles indicates that Al_3Ti presented nucleation, growth and coarsening. The electron diffraction pattern included in Figure 4a corroborated the formation of Al_3Ti. On the other hand, Figure 4c shows the interface Al-Al_3Ti, which is clean and without the formation of precipitates or other reaction products. This kind of well bonded interface favors strength and ductility. Finally, Figure 4d shows the formation of α-Al_2O_3 particles of ~100 nm in size, another reaction product of Equation 16. XRD studies of these authors showed that part of the TiO_2 still remained in the final composite, completing the observed in Equation 16.

The reduction of TiO_2 to Ti was found by Ghanaraja et al.[155] for a composite with TiO_2 contents from 3 to 12 wt.% manufacturing by stir casting at 900 °C. These authors added 2% Mg to Al for increasing wettability of the reinforcement. They found that the resulting composite was Al (Mg,Ti)-Al_2O_3 (TiO_2), starting from a matrix of Al-Mg-Ti alloy reinforced with oxide particles consisting of un-reacted TiO_2 and Al_2O_3. Other expected phases due to this reaction are $MgAl_2O_4$, MgO, $MgTi_2O_4$ and Al_2TiO_5, which act as reinforcements in the matrix. In presence of Mg the following reaction is reported for the formation of MgO[156]:

$$TiO_{2(s)} + 3Al_{(l)} + 2Mg_{(l)} = Al_3Ti_{(s)} + 2MgO_{(s)} \qquad (17)$$

The Al-TiO_2 system reaction has been used for the in-situ fabrication by powder metallurgy of Al_3Ti and Al_2O_3 particles[154]. The use of an Al-Si alloy modified the reaction products, being them Ti_5Si_3 besides Al_2O_3[157]:

$$3TiO_{2(s)} + 4Al_{(l)} + 1.8Si_{(l)} = 2Al_2O_{3(s)} + 0.6Ti_5Si_{3(s)} \qquad (18)$$

These products can be also obtained by two reactions:

$$3TiO_{2(s)} + 4Al_{(l)} = 2Al_2O_{3(s)} + 3Ti_{(l)} \qquad (19)$$

$$3Ti_{(l)} + 1.8Si_{(l)} = 0.6Ti_5Si_{3(s)} \qquad (20)$$

Otherwise, for Al alloys with Cu it has been reported the presence of Al_5CuTi_2, Al_4Cu_9 and Al_3Ti as reaction products[158]. This shows that as was observed for Al_2O_3, TiO_2 also presents reaction products with Cu, but works reported in literature are few. Again, more research is needed for the interaction of this alloying element with oxide reinforcements in Al matrix composites.

3.4. ZrO_2

Zirconium dioxide (Zirconia, ZrO_2) is considered one of the most important ceramic materials for manufacturing MMC, although its density is considerably high (5.68 gcm^{-3}). It presents high flexural strength, good fracture toughness and

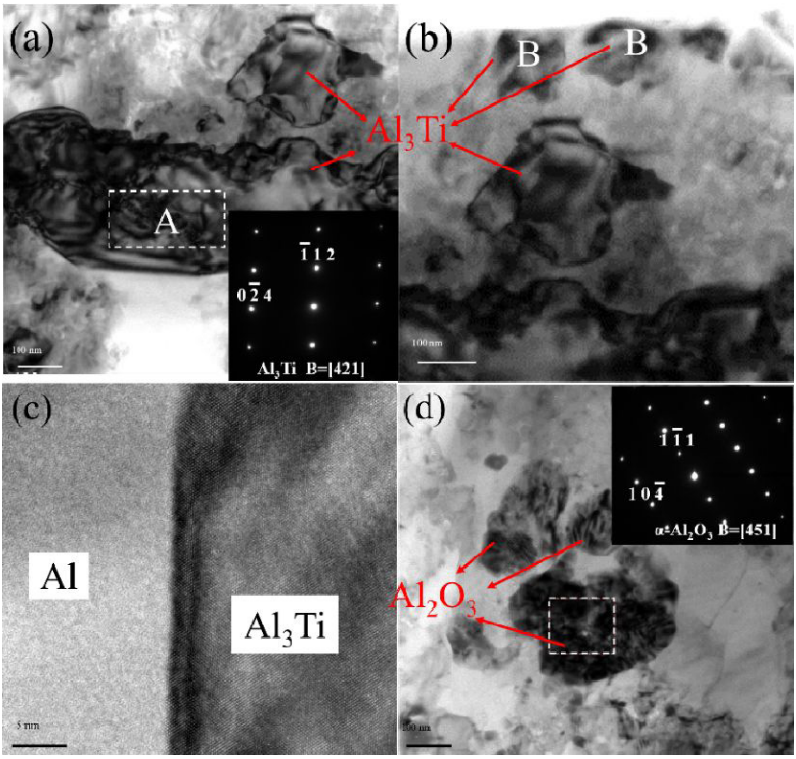

Figure 4. TEM images of: (a) Al_3Ti and its SAD pattern of region A, (b) Al_3Ti with nanometric size (B), (c) HRTEM image of the interface Al-Al_3Ti, and (d) α-Al_2O_3 particles of nanometric size and the corresponding SAD pattern. (Reproduced with permission from[154]).

stability at high temperature. Also has wear and corrosion resistance, reinforcing Al alloys in applications such as abrasives, support material for catalysis, ceramic tubes, connecting rods, and thermal insulations[27,159]. Different reactions are reported between zirconia and Al. Zhu et al.[160] reported that at 750 °C Al_3Zr phase could be formed through the following exothermic reaction:

$$13Al_{(l)} + 3ZrO_{2(s)} = 2Al_2O_{3(s)} + 3Al_3Zr_{(s)} \qquad (21)$$

A similar reaction has been reported at temperatures higher than 800 °C, but without the formation of Al_3Zr[161]:

$$4/3Al_{(l)} + ZrO_{2(s)} = 2/3Al_2O_{3(s)} + Zr_{(l)} \qquad (22)$$

Rostami and Tajall[162] also reported the formation of Al_3Zr in an Al-9.7Si-2.1Cu-1.0Mg alloy reinforced with ZrO_2 and Al_2O_3, obtained by stir melting at 750 °C. These authors revealed that Al_3Zr remained undissolved even at elevated temperatures, and its presence enhanced the wettability of Al_2O_3 particles obtained through Equation 22, which also reinforce the material. Besides, the presence of Al_3Zr reduced porosity and led to increase tensile and yield strengths. These authors also identified precipitates as $(Al,Si)_3Zr$. No other precipitates or interfacial products were reported although Mg and Cu are present in the matrix, only the precipitates which are characteristics for this alloy system (i.e. Al_2Cu, $Al_5Cu_2Mg_8Si_6$, Mg_2Si). Baghchesara et al.[163] found Si nucleation on the surface of ZrO_2 particles for Al-7.23Si alloys reinforced with 5, 10 and 15 vol. % ZrO_2 using stir casting at 950 °C, but Si-rich products were not detected. These authors agree in the fact that Al_3Zr acts as hard pinning points in the matrix inhibiting dislocation motion, affecting the strength of the composite[164]. Moya et al.[161] also studied an Al-5.2Si-3.5Cu-0.5Mg alloy, but the presence of Cu and Mg did not cause the formation of other phases.

Related to microstructural modifications, Sharma et al.[165] studied the effect of ZrO_2 nanoparticles added into a molten Al-12Si-20Cu alloy at 750 °C, and homogenized at 1100 °C. They found that the addition of ZrO_2 led to affect the morphology of the second phases present in the alloy, but did not cause the formation of Zr-rich phases. Second phases were Si particles, Al_2Cu, and eutectics of Al-Si, Al-Cu, and Al-Si-Cu. Daoud et al.[166] also found an important modification of the microstructure due to the addition of 5%ZrO_2 particles with irregular shapes, as it can be observed in Figure 5a,b. This figure shows that silicon phase in the matrix of the composites (Figure 5b) is significantly finer than that of the unreinforced alloy. Khalili et al.[81] studied an Al-1Mg-0.55Si-0.26Cu (in wt.%) alloy reinforced with 3 and 6% of 30 µm in diameter ZrO_2 particles, stir melted at 700 °C. They found that Mg acted as a surface-active agent, increasing the wettability of the ZrO_2 particles. Besides reported the presence of Mg_2Si, Al_8Fe_2Si, CuO, and Al_2O_3, but no chemical reactions matrix-ZrO_2 to originate new phases. As can be observed in Figure 5c-e, the addition of ZrO_2 particles to this alloy led to significantly decrease the grain size, attributed to the presence of ZrO_2 as nucleation sites. It could be thought that the increase in the ZrO_2 percentage from 3 to 6 wt.% would originate a reduction in the grain size, but its average increased from 62 to 93 µm due to the agglomeration of the ZrO_2 particles, decreasing the surface

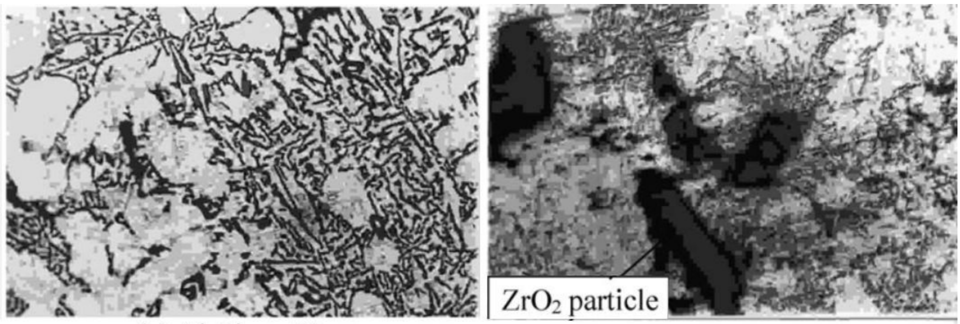

(a) Al-Si 50 µm (b) Al-Si+ZrO₂ 50 µm

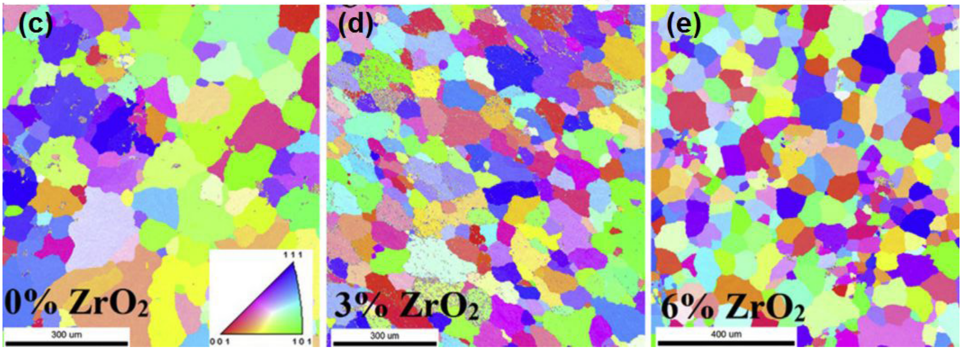

Figure 5. OM images of the microstructures for an Al–Si alloy (a), and for the same alloy reinforced with 5% of ZrO_2 particles (b). (Reproduced with permission from[166]). (c-e) Inverse pole maps for: c) unreinforced 6061 alloy, d) 6061 alloy reinforced with 3 wt.% ZrO_2, and e) 6061 alloy reinforced with 6 wt.% ZrO_2. (Reproduced with permission from[81]).

area of the particles. Agglomeration is derived from the increase in the viscosity of the melt, also originating pores and other detrimental defects for the mechanical properties. These results show that care must be taken in the correct selection of the size and percentage of the reinforcement.

Although the above presented works did not show reactions between Mg and ZrO_2, Liu et al.[167] reported the formation of other phases with the presence of Mg. They studied a ZrO_2/Al-10.8Mg composite manufactured at 910 °C, and found an interfacial reaction which led to the formation of Al_3Zr, $Zr_{0.875}Mg_{0.125}O_{1.875}$ and $Al_{0.1}Zr_{0.9}O_{1.95}$, being the Mg content the highest among all the elements present at the interface. This can be observed in the SEM image and EDS mappings of Figure 6, where a ZrO_2 particle is surrounded by a reaction layer rich in Mg and O, demonstrating the formation of MgO according to the following reaction due to the high Mg content in the alloy:

$$2\,Mg_{(l)} + ZrO_{2(s)} = 2\,MgO_{(s)} + Zr_{(l)} \tag{23}$$

The formation of polygonal Al_3Zr in the outer area of the reaction layer is also corroborated in Figure 6[167]. This reaction product is obtained through the following reaction, starting from Equation 23:

$$Al_{(l)} + Zr_{(l)} = Al_3Zr_{(s)} \tag{24}$$

Other reactions products have been reported for composites obtained with alloys presenting high Mg and Si contents. Guo et al.[168] found the presence of different Zr-rich phases during the pressureless infiltration of 30 vol.% of mixtures Al_2O_3-ZrO_2 of weight ratios 1:9, 3:7, 5:5, 7:3 and 9:1 with an Al-12Si-10Mg alloy. They observed multiple chemical reactions, being the main reaction products $(Al_{1-m},Si_m)_3Zr$, Al_2O_3 and $ZrSi_2$. On the other hand, Gao et al.[169] reported that with the increase of Si in an Al-Si-Zr alloy, the primary phase changed from Al_3Zr to (Al,Zr,Si) and further to $ZrSi_2$. These phases increased the compressive strength but decreased toughness.

The above presented results show that the addition of Cu to Al alloys reinforced with ZrO_2 does not cause the formation of any reaction product, while Si and Mg additions lead to reactions involving these elements, obtaining a wide variety of reaction products. Although these reactions are generally reported as beneficial for the mechanical properties of the composites, works found in literature for Al matrices with Si or Mg are relatively few, even for the case of Mg. This element as wetting improver and its reactions with the reinforcements presented in the previous sections were more reported than for ZrO_2.

3.5. Y_2O_3

Yttrium oxide (yttria, Y_2O_3), exhibits remarkable stability against liquid aluminum. Nevertheless, different research works report the formation of reaction products through the following reactions[128,170,171]:

$$Y_2O_{3(s)} + 2Al_{(l)} = Al_2O_{3(s)} + 2Y_{(l)} \tag{25}$$

$$Y_2O_{3(s)} + Al_{(l)} = AlYO_{3(s)} + Y_{(l)} \tag{26}$$

Examples of the formation of $YAlO_3$ due to reaction of Equation 26 were presented in the works of Barzilai et al.[170,171] for the study of the metal-Y_2O_3 interface at 1423 K, using Al, Al-Cu and Al-Cu-Y matrices. They reported that Y_2O_3 decomposed and Y was transferred into the molten metal,

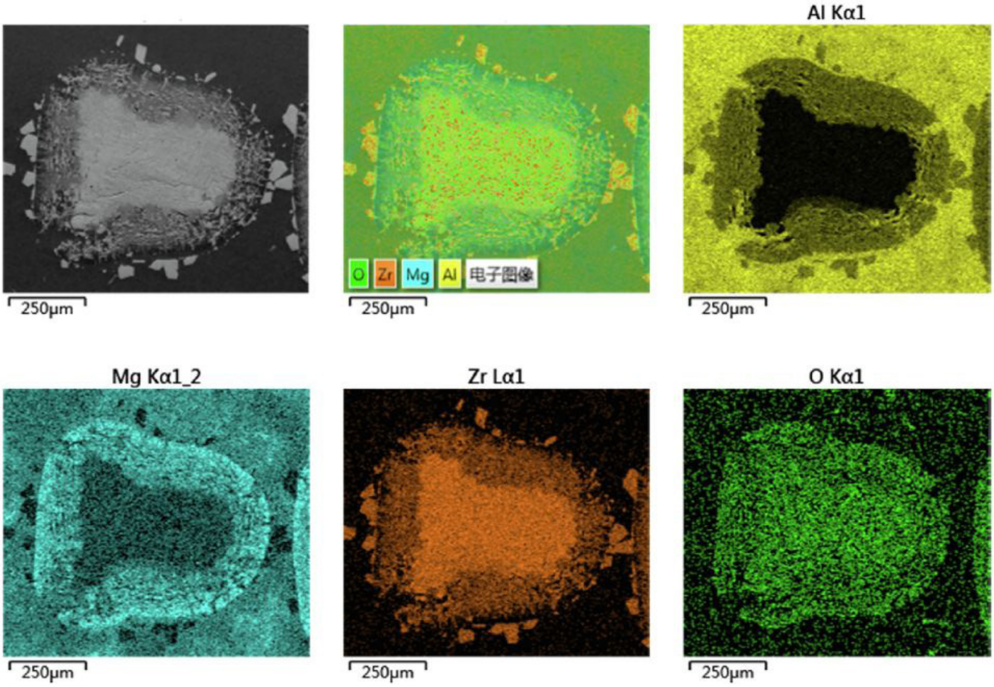

Figure 6. SEM image of a ZrO_2 block-like phase and EDS mappings showing the presence of a MgO layer and Al_3Zr particles in the outer region. (Reproduced with permission from[167]).

depending the reaction extension on the alloying elements content. If Y content in the alloy is high (>10 at.%) the formation of $AlYO_3$ decreased while high Cu contents (>10 at.%) decreased wettability and $AlYO_3$formation. This can be observed in Figure 7a for an Al pure matrix, where Y_2O_3 almost disappeared due to the formation of $AlYO_3$. The addition of 15 at. % Y led to a decrease in the thickness of the $AlYO_3$ layer (Figure 7b), while an Y content of 75% completely avoided its formation, being obtained Y_2O_3. This oxide is different from the initial Y_2O_3 due to stoichiometric changes[171]. These results show that the interactions between matrices and reinforcements are complex, not only obtaining different reaction products but also modifying the starting reinforcements without the detection of new products, as the case of the stoichiometric modification of Y_2O_3.

For the Al-yttria system it has been also reported that when Al oxidizes according to Equation 25 and 26, three different reactions can occur, which are[172]:

$$2Y_2O_{3(s)} + Al_2O_{3(s)} = Y_4Al_2O_{9(s)} \tag{27}$$

$$Y_4Al_2O_{9(s)} + Al_2O_{3(s)} = 4YAlO_{3(s)} \tag{28}$$

$$3YAlO_{3(s)} + Al_2O_{3(s)} = Y_3Al_5O_{12(s)} \tag{29}$$

Otherwise, Al_2Y as reaction product was reported by Yu et al.[173] due to the interfacial reaction in a 6061Al alloy reinforced with Al_2O_3 particles coated with Y_2O_3. This product, different of the above mentioned, improved wettability and bonding strength of the interface, leading to better mechanical properties. Al_2Y was originated due to the reaction between Al liquid and Y_2O_3:

$$Y_2O_{3(s)} + 3Al_{(l)} = Y_2Al_{(s)} + Al_2O_{3(s)} \tag{30}$$

Kim et al.[174] analyzed the effect of adding Y_2O_3 to pure aluminum (99% purity) inside the mold at 900 °C, and found that Y_2O_3 nanoparticles were uniformly distributed in the matrix, not reporting particles degradation or reactions with molten Al. The presence of 2% of Y_2O_3 led to increase hardness by 1.2 times and tensile strength by 1.55 times. Zhang et al.[175] used 1% of Y_2O_3 for reinforcing pure Al, manufacturing the composite by conventional casting, and showing that the dispersed yttria particles are effective in enhancing both the mechanical properties and corrosion resistance of the Al matrix.

The presence of alloying elements can lead to the formation of different interfacial compounds. Moussa et al.[176] reported another reaction for an Al-7.36Si-0.23Mg-0.103Cu alloy at which was added Al−30wt.%Y_2O_3 powder when melt reached 750 °C. This led to the formation of Al_3Y, which segregated at the edge of eutectic Si restricting its growth and leading to its modification. These authors did not report the formation of Y_2SiO_5, but the EDS presented in their research could indicate its formation. Bouaeshi and Li[177] also used premixed powder of Al−Y_2O_3 followed by melting in an arc-melting furnace. Using XRD they demonstrated the formation of Al_3Y, while this technique and SEM/EDS examinations showed the absence of Y_2O_3. This suggests that this phase completely decomposed due to the high temperature (up to 3700 °C), which is higher than the melting point of yttria. Hardness, mechanical and electrochemical properties of Al were improved due to the Al_3Y phase, residual yttrium in Al matrix and finer microstructure. Figure 8a-b presents backscattered SEM images of these composites studied by Bouaeshi and Li[177], where microstructures consisted of aluminum dendrites and Y-rich eutectic domains. As can be seen, the increase in the Y_2O_3 addition made the microstructure finer. Besides, Y_2O_3 melted or decomposed during the manufacturing process due to the high temperature, forming Al_3Y according to Equation 26:

$$Y_2O_{3(s)} + 6Al_{(l)} = 2Al_3Y_{(s)} + 3/2O_{2(g)} \tag{31}$$

Al_3Y particles can be better observed in the SEM image of Figure 8c arrowed B (at higher magnifications). The XRD diffractogram of Figure 8d shows the increase in the intensity of the peaks for this phase with the increase in the Y_2O_3 quantity used in the manufacturing process, and the absence of Y_2O_3 due to the reaction of Equation 25.

Oliveira et al.[178] studied the interaction of a sintered mixture of various ceramics ($90Si_3N_4$–$5Y_2O_3$–$5Al_2O_3$) with molten Al, and found that sintering originated the formation of Y_2SiO_5. Then, it could be thought that if Y_2O_3 is in contact with a molten Si-rich Al alloy this compound could be also formed. This could confirm the above commented

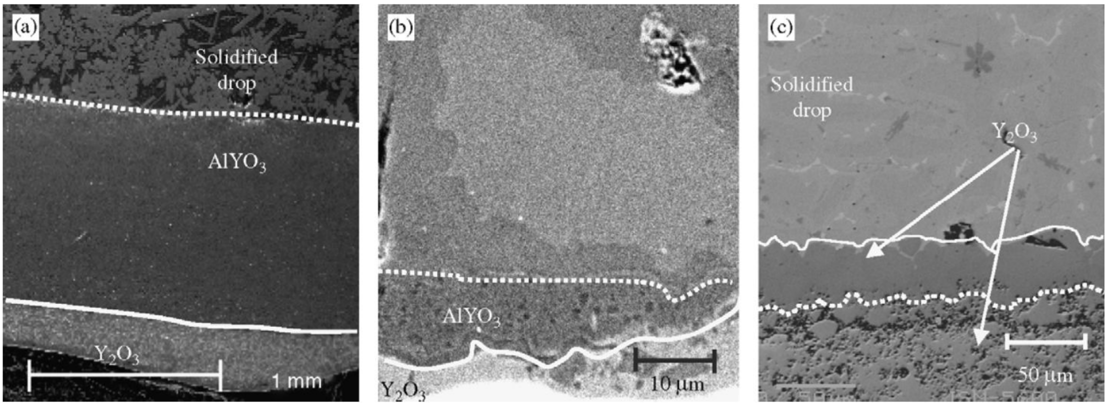

Figure 7. SEM images for Y_2O_3/Al matrix interfaces for: (a) Pure Al matrix, (b) Al-15Y matrix, and (c) Al-75Y matrix. (Reproduced with permission from[171]).

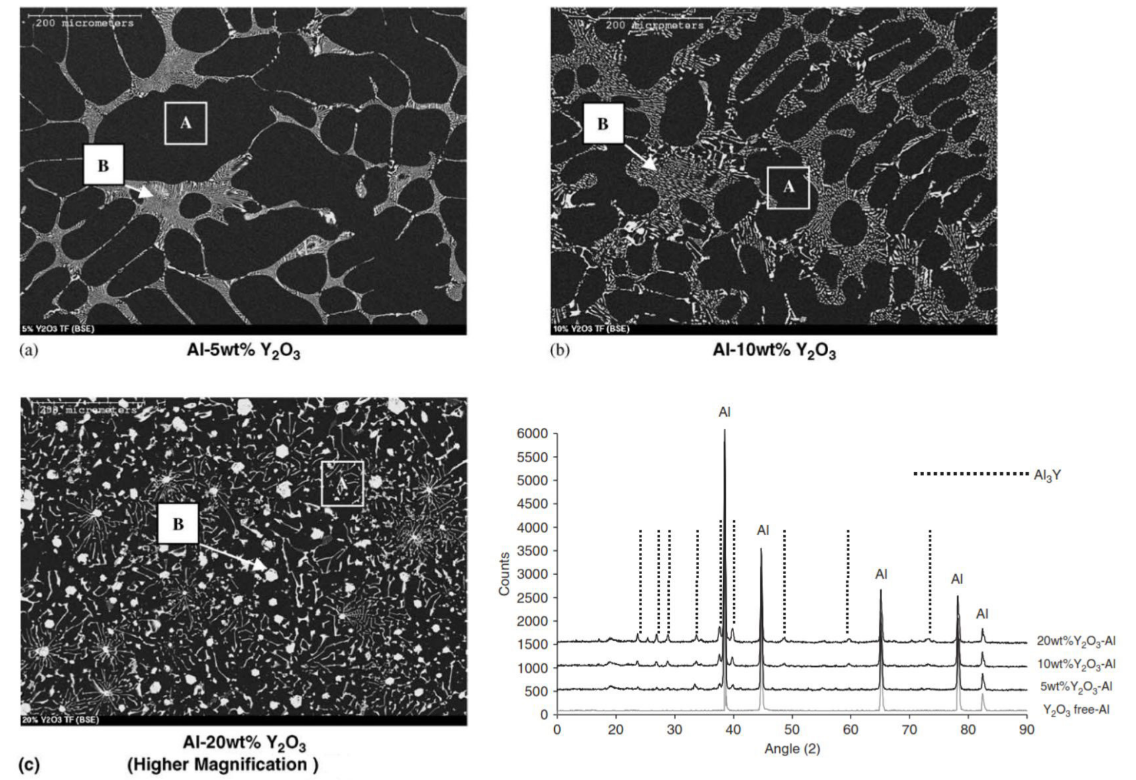

Figure 8. SEM images of Al-Y_2O_3 composites with: a) 5 wt.% Y_2O_3, b) 10 wt.% Y_2O_3, and 15wt.% Y_2O_3. (d) XRD diffractograms of unreinforced Al and with different contents of Y_2O_3. (Reproduced with permissions from[177]).

report about EDS findings in the work of Moussa et al.[176], and shows that research about this topic is insufficient and needs more attention.

Corrosion of composite materials quite often begins with the reaction of the reinforcement material, being in general the composites more susceptible to corrosion attack than the matrix alloy. Nevertheless, Anaee[179] found that the corrosion resistance of an Al-Si-Cu alloy reinforced with 1% of Y_2O_3 is higher than the unreinforced alloy, although if Y_2O_3 content is increased the corrosion resistance is not improved. This author did not analyze the microstructure of the composites, being impossible to conclude if Y_2O_3 particles remains without significant changes or if another compound was obtained.

Few works were found in literature about the effect of Mg for Y_2O_3 reinforced Al alloys, but it has been reported that Y_2O_3 exhibits better stability in molten magnesium than other oxide reinforcements such as alumina and zirconia[180]. Divakar et al.[181] studied an Al-Mg alloy reinforced with 4%Y_2O_3 processed at 600 °C, and found a relatively uniform distribution of reinforced particles. Y_2O_3 presented good interfacial integrity without any damage. These particles significantly increased hardness and tensile strength of the composite.

The above presented results show that the information related to the effect of Si, Cu and Mg on possible reactions of Al-Y_2O_3 composites is limited. From the works about this system found in literature it can be concluded that Y_2O_3 is less reactive than other oxide reinforcements, being only reported reaction products rich in Si. Although Cu and/or Mg additions did not lead to the formation of interfaces they could affect wettability and the distribution of the reinforcements.

3.6. CeO_2

Cerium Oxide (Ceria, CeO_2) has high stability at elevated temperatures, good behavior against mechanical abrasion and is a cathodic inhibitor. Nevertheless, its study as reinforcement of Al alloys has been limited[182], being used mainly as coating, similar to the case of BN[183]. Skrzekut et al.[184,185] studied mechanical alloying of Al with 9.2% of CeO_2 particles at annealing temperature ≤ 773 K, reporting high thermal stability of CeO_2. For an Al-4.88Mg matrix they detected the decomposition of CeO_2 particles forming Al_4Ce and Al-Mg rich oxides as reaction products. This reaction did not occur for the system Al-CeO_2, but the addition of Mg led to the reduction of CeO_2 like for other MeO particles resulting in Al_xMe_y (Me=metal). The spinel $Mg_{0.4}Al_{0.6}Al_{1.8}O_{0.4}$ was also reported in this work. This reaction could be deduced from similar reactions in systems such as AlMg-SiO_2 or AlMg-TiO_2, being as follows:

$$2CeO_{2(s)} + 10Al_{(l)} + Mg_{(l)} = 2Al_4Ce_{(s)} + MgAl_2O_{4(s)} \qquad (32)$$

Example of the formation of Al_4Ce can be observed in Figure 9a-b from the works of Skrzekut et al.[184,185], were the TEM images and the SAD (Selected Area Diffraction) patterns

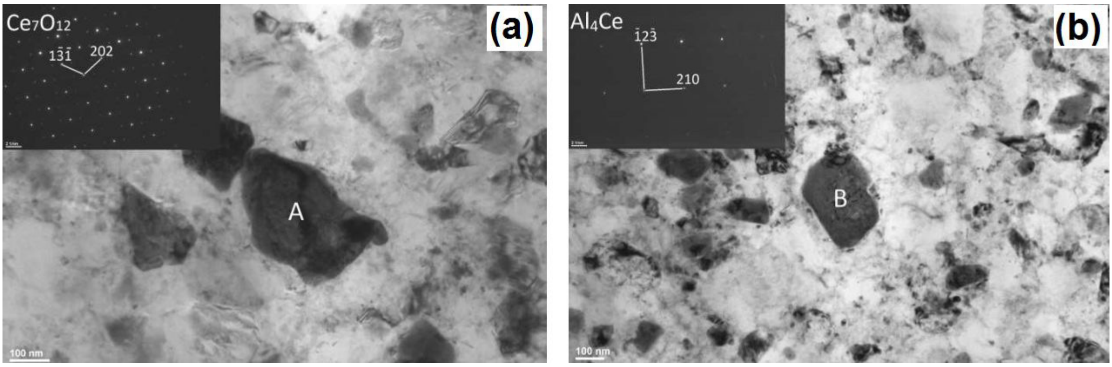

Figure 9. TEM images of an AlMg-CeO_2 composite where the presence of Ce_7O_{12} and Al_4Ce nanoparticles can be observed, corroborated by their SADPs. (Reproduced with permissions from[184]).

reveal the presence of Ce_7O_{12} as an intermediate product of the reduction of CeO_2 (Figure 9a). The end of this reaction led to the nucleation and growth of Al_4Ce (Figure 9b). The use of these techniques revealed the similarities of these particles, being necessary this kind of studies for their identification. This reaction took place during mechanical alloying at 673 K, but the presence of Al_4Ce significantly increased when the composite was re-melted at 973 K, almost completely decomposing CeO_2. This was corroborated by XRD studies, which also revealed that $MgAl_2O_4$ peaks were less intense, meaning that after the complete reaction instead of Equation 32 the formation of small quantities of oxides such as MgO or Al_2O_3 could occur. These authors mentioned that other phases such as $CeO_{1.66}$ and Ce_4O_7 could be also present after re-melting.

Xue et al.[56] reported the formation of AlSiCe and Al_4Ce for an Al-6.97Si-0.36Mg alloy reinforced with 1% CeO_2. AlSiCe had needle-like or block irregular morphologies and bad bonding with the matrix, which decreased the mechanical properties. The formation of AlSiCe originated the decrease in the concentration of Ce in grain and inter-dendritic boundaries, also leading to modify eutectic Si.

The bibliographic search of possible reactions between CeO_2 and aluminum alloys revealed that reaction products were only obtained when Si or Mg were present, while there were not found reports of reactions for pure Al matrices. The effect of Cu on the matrix-reinforcement interactions for these composites was also not found. This shows again, as for Al-Y_2O_3 composites, the limited information related to possible interfacial reactions in these systems, being necessary new research about this important topic. This lack of information is even more critical for the case of CeO_2.

3.7. MgO

Magnesium oxide (MgO, magnesia) has a density of 3.58 gcm^{-3} and a melting point of 2800°C. It also has elevated Young Modulus (320 GPa), compressive strength and hardness. Also present excellent thermodynamic stability and high wettability with aluminum[186]. Al-MgO composites are used where light weight and high strength-to-weight are needed[187]. For the case of the interaction between molten Al and MgO, the following reaction has been reported[128,188]:

$$3MgO_{(s)} + 2Al_{(l)} = Al_2O_{3(s)} + 3Mg_{(l)} \tag{33}$$

As was already observed for the additions of Si to Al alloys reinforced with SiO_2, and Y to alloys reinforced with Y_2O_3, adding to the matrix high contents of the same alloying element which constitutes the oxide reinforcement allows to avoid or diminish the formation of interfacial reactions. For example, Mohammed and Gamal[189] reported the absence of any intermetallic formation in an Al1100 alloy reinforced with 0-4 wt.% of MgO casting at 750 °C. Yar et al.[190] found that the addition of 1.5 wt.% of MgO particles to an Al-7.23Si-0.32Fe-0.18Cu-0.38Mg A356.1 alloy manufactured at 850 °C led to improve properties such as hardness, strength and toughness. For these conditions, no reactions products were observed. Lin et al.[191] also found that the use of MgO as coating avoided the interfacial reaction between an Al-6Mg-0.4Si-0.1Cu alloy and glass microspheres (SiO_2) used in syntactic foams manufactured at 850 °C. These authors reported a large amount of $MgAl_2O_4$, Si and Mg_2Si at the interfaces when there were used spheres without MgO coating. Calin and Citak[192] studied an Al matrix with 0, 1, 2, 3 and 4% Mg reinforced with MgO by infiltration, and reported that when Mg content and temperature of matrix increased the infiltration process was easier. They found the formation of the spinel $MgAl_2O_4$ phase, which facilitated the infiltration of Al. The formation of this phase could be directly from the melt due to the reaction between Al, Mg and O_2; or from the interaction MgO-molten alloy. Sun et al.[193] used TEM to study the interactions between a MgO substrate and molten Al, and found the formation of an intermediate layer of and $MgAl_2O_4$, as can be observed in Figure 10a. Figures 10b, c show the HRTEM analysis of this layer along the [001] zone axis of MgO, where the lattice structure defined by different planes can be observed. Fast Fourier Transformation (FFT) analysis corroborated that the intermediate layer is $MgAl_2O_4$, with a face-centered cubic (FCC) structure corresponding to the planes (400) and (220). These images reveal that orientation relationships between phases are [001] (400) $MgAl_2O_4$// [001] (200) MgO and [001] (220) $MgAl_2O_4$//[001] (220) Al.

For Al matrices with the presence of Si it is reported that the reaction with MgO could lead to the formation of $MgAl_2O_4$ and Mg_2SiO_4, although only it is possible for very high Si contents (mass ratios of MgO:Al:Si=70:15:15) and high mixture temperatures (1450 °C)[194]. The formation of

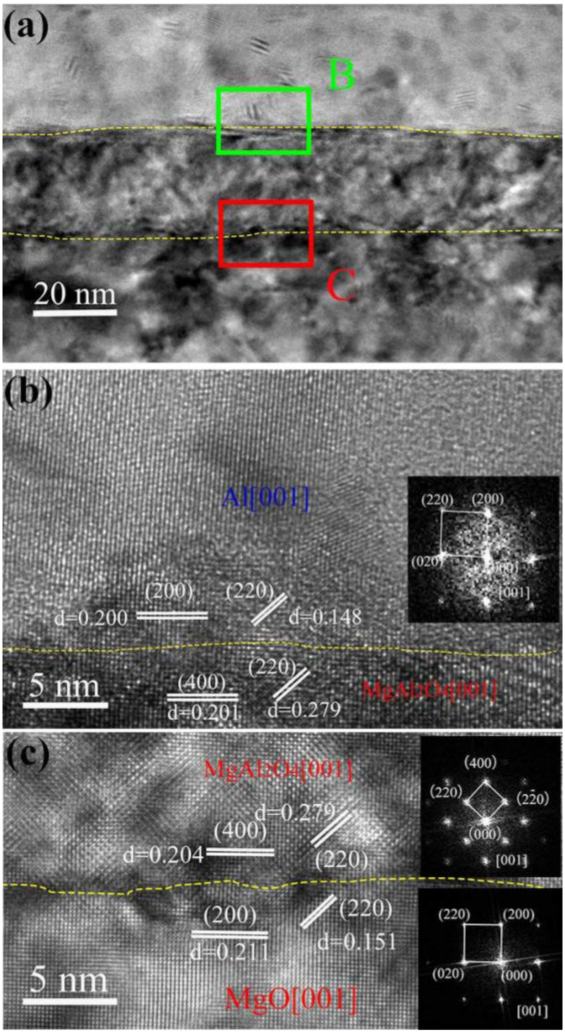

Figure 10. (a) TEM image of an Al(up)/MgO(down) composite with an $MgAl_2O_4$ interfacial layer. (b) HRTEM image of the Al/$MgAl_2O_4$ interface, corresponding to frame (B). (c) HRTEM image of the $MgAl_2O_4$/MgO interface, corresponding to frame (C). FFTs are included for each phase. (Reproduced with permissions from[194]).

intermetallics between MgO and Cu or the effect of this element was not found for these composites.

As can be seen for composites of the system MgO-Al alloys the most important and studied alloying element is Mg, in this case due to its influence avoiding interfacial reactions.

4. Summary

After the analysis of the interactions between oxide reinforcements and Al matrices with Si, Cu and/or Mg as alloying elements, it can be concluded that research in literature about this topic is insufficient. It is generally accepted that the increase in the reinforcement volume fraction modifies the microstructure and decreases the grain size. Nevertheless, it is essential an adequate manufacturing process in order to avoid reinforcement agglomerations that could avoid grain refinement. Related to interfacial reactions, the conditions for their occurrence are different and highly dependent on temperature and composition of the matrix. It is necessary an individual study of each combination reinforcement-matrix, mainly including the alloying elements content. For some oxides used as reinforcements such as Al_2O_3 and SiO_2 the reactions and interactions are well studied, but for others the information is limited or inexistent, as the case of CeO_2 and Y_2O_3. Interfacial reactions could lead to the diffusion of elements, which may decrease the precipitation in the region near the interface if the alloying element segregates to the interface; or generate new precipitates if an element diffuses from the reinforcement to the matrix. In general, Mg is the most studied element, being also who has the highest effect on interfacial reactions. This could be attributed to the high reactivity of this element and to its role as wettability improver when is added to Al matrices. Among the reactions products, spinel $MgAl_2O_4$ phase was the most reported because it is present for all the oxides except ZrO_2 and Y_2O_3. The presence of Si in interfacial products was lower, but this element was found in all the oxides forming interfacial compounds or precipitates. On the other hand, the effect of Cu was barely found in literature, with few reaction products, only for Al_2O_3 and TiO_2. Besides, it was found that an effective way for minimizing the reduction reaction of an oxide reinforcement is adding to the alloy the same element of the oxide.

5. Acknowledgements

I. Alfonso acknowledges the financial support from PASPA DGAPA-UNAM and SEP CONACYT 285215 project. The support of Departamento de Ingeniería de Procesos e Hidráulica, Universidad Autónoma Metropolitana-Iztapalapa is also acknowledged.

6. References

1. Hatch JE. Aluminum: properties and physical metallurgy. Metals Park: American Society for Metals; 1984.
2. Hirsch J, Skrotzki B. Aluminium alloys: the physical and mechanical properties. Weinheim: Wiley-VCH; 2008.
3. Rana RS, Purohit R, Das S. Reviews on the influences of alloying elements on the microstructure and mechanical properties of aluminum alloys and aluminum alloy composites. Int J Sci Res. 2012;2:1-7.
4. Zeren M. Effect of copper and silicon content on mechanical properties in Al–Cu–Si–Mg alloys. J Mater Process Technol. 2005;169(2):292-8.
5. Lee CD. Effect of damage evolution of Si particles on the variability of the tensile ductility of squeeze-cast Al–10%Si–2%Cu–0.4%Mg alloy. Mater Sci Eng A. 2010;527:3144-50.
6. Dighe MD, Gokhale AM, Horstemeyer MF, Mosher DA. Effect of strain rate on damage evolution in a cast Al-Si-Mg base alloy. Metall Mater Trans, A Phys Metall Mater Sci. 2000;31:1725-31.
7. Zeren M, Karakulak E, Gümü S. Influence of Cu addition on microstructure and hardness of near-eutectic Al-Si-xCu-alloys. Trans Nonferrous Met Soc China. 2011;21:1698-702.
8. Ma Z, Samuel AM, Samuel FH, Doty HW, Valtierra S. A study of tensile properties in Al-Si-Cu and Al-Si-Mg alloys: effect of β-iron intermetallics and porosity. Mater Sci Eng A. 2008;490(1-2):36-51.
9. Wang G, Bian XF, Wang WM, Zhang JY. Influence of Cu and minor elements on solution treatment of Al–Si–Cu–Mg cast alloys. Mater Lett. 2003;57:4083-7.

10. Caceres CH, Davidson CJ, Griffiths JR, Wang QG. The effect of Mg on the microstructure and mechanical behavior of Al-Si-Mg casting alloys. Metall Mater Trans, A Phys Metall Mater Sci. 1999;30:2611-8.
11. Yıldırım M, Özyürek D. The effects of Mg amount on the microstructure and mechanical properties of Al–Si–Mg alloys. Mater Des. 2001;51:767-74.
12. Salleh MS, Omar MZ, Syarif J. The effects of Mg addition on the microstructure and mechanical properties of thixoformed Al–5%Si–Cu alloys. J Alloys Compd. 2015;621:121-30.
13. Samuel FH, Ouellet P, Samuel AM, Doty HW. Effect of Mg and Sr additions on the formation of intermetallics in Al-6 wt pct Si-3.5 wt pct Cu-(0.45) to (0.8) wt pct Fe 319-type alloys. Metall Mater Trans, A Phys Metall Mater Sci. 1998;29:2871-84.
14. Mohamed AMA, Samuel FH. Al kahtani S. Influence of Mg and solution heat treatment on the occurrence of incipient melting in Al–Si–Cu–Mg cast alloys. Mater Sci Eng A. 2012;543:22-34.
15. Samuel FH. Incipient melting of $Al_5Mg_8Si_6Cu_2$ and Al_2Cu intermetallics in unmodified and strontium-modified Al-Si-Cu-Mg (319) alloys during solution heat treatment. J Mater Sci. 1998;33:2283-97.
16. Alfonso I, Maldonado C, Gonzalez G, Bedolla A. Effect of Mg content and solution treatment on the microstructure of Al-Si-Cu-Mg alloys. J Mater Sci. 2006;41:1945-52.
17. Casas BY, Carranza JC, Figueroa IA, González JG, Hernández O, Béjar L, et al. Fractal and conventional analysis of Cu content effect on the microstructure of Al-Si-Cu-Mg Alloys. Mater Res. 2020;23:e20190666.
18. Alfonso I, González G, Lara G, Rodríguez M, Domínguez M, Téllez MG, et al. Fractal analysis of the heat treatment response for multiphase Al alloys. Mater Res. 2016;19:628-39.
19. Farkoosh AR, Pekguleryuz M. Enhanced mechanical properties of an Al–Si–Cu–Mg alloy at 300 °C: Effects of Mg and the Q-precipitate phase. Mater Sci Eng A. 2015;21:277-86.
20. Farahany S, Nordin NA, Ourdjini A, Abu Bakar T, Hamzah E, Idris MH, et al. The sequence of intermetallic formation and solidification pathway of an Al–13Mg–7Si–2Cu in-situ composite. Mater Charact. 2014;98:119-29.
21. Nordin NA, Farahany S, Ourdjini A, Bakar TAA, Hamzah E. Refinement of Mg_2Si reinforcement in a commercial Al–20%Mg_2Si in-situ composite with bismuth, antimony and strontium. Mater Charact. 2013;86:97-107.
22. Azarbarmas M, Emamy M, Rassizadehghani J, Alipour M, Karamouz M. The influence of beryllium addition on the microstructure and mechanical properties of Al–15%Mg_2Si in-situ metal matrix composite. Mater Sci Eng A. 2011;528:8205-11.
23. Aravind M, Yu P, Yau MY, Dickon HLN. Formation of Al_2Cu and AlCu intermetallics in Al(Cu) alloy matrix composites by reaction sintering. Mater Sci Eng A. 2004;380:384-93.
24. Dinaharan I, Balakrishnan M, Selvam JDR, Akinlabi ET. Microstructural characterization and tensile behavior of friction stir processed AA6061/Al_2Cu cast aluminum matrix composites. J Alloys Compd. 2019;781:270-9.
25. Ibrahim MF, Samuel E, Samuel AM, Al-Ahmari AMA, Samuel FH. Metallurgical parameters controlling the microstructure and hardness of Al–Si–Cu–Mg base alloys. Mater Des. 2011;32:2130-42.
26. Zheng Y, Xiao W, Ge S, Zhao W, Hanada S, Ma C. Effects of Cu content and Cu/Mg ratio on the microstructure and mechanical properties of Al–Si–Cu–Mg alloys. J Alloys Compd. 2015;649:291-6.
27. Samal P, Pandu RV, Meher A, Manas MM. Recent progress in aluminum metal matrix composites: a review on processing, mechanical and wear properties. J Manuf Process. 2020;59:131-52.
28. Senthil S, Raguraman M, Manalan DT. Manufacturing processes & recent applications of aluminium metal matrix composite materials: a review. Mater Today. 2021;45(7):5934-8.
29. Ramnath BV, Elanchezhian C, Annamalai RM, Aravind S, Atreya TSA, Vignesh V, et al. Aluminium metal matrix composites - a review. Rev Adv Mater Sci. 2014;38:55-60.
30. Ge D, Gu M. Mechanical properties of hybrid reinforced aluminum based composites. Mater Lett. 2001;49(6):334-9.
31. Zhang WX, Li LX, Wang TJ. Interface effect on the strengthening behavior of particle-reinforced metal matrix composites. Comput Mater Sci. 2007;41(2):145-55.
32. Lasagni F, Degischer HP. Enhanced Young's modulus of Al-Si alloys and reinforced matrices by Co-continuous structures. J Compos Mater. 2010;44(6):739-55.
33. Simões S, Viana F, Reis MAL, Vieira MF. Improved dispersion of carbon nanotubes in aluminum nanocomposites. Compos Struct. 2014;108:992-1000.
34. Mitra R, Mahajan YR. Interfaces in discontinuously reinforced metal-matrix composites. Def Sci J. 1993;43(4):397-418.
35. Mitra R, Mahajan YR. Interfaces in discontinuously reinforced metal matrix composites: an overview. Bull Mater Sci. 1995;18(4):405-34.
36. Miracle DB, Donaldson SL, editors. ASM handbook: volume 21: composites. Ohio: ASM International; 2001.
37. Mavhungu ST, Akinlabi ET, Onitiri MA, Varachia FM. Aluminum Matrix Composites for industrial use: advances and trends. Procedia Manufacturing. 2017;7:178-82.
38. Sharma AK, Bhandari R, Aherwar A, Rimašauskienė R, Pinca-Bretotean C. A study of advancement in application opportunities of aluminum metal matrix composites. Mater Today. 2020;26(2):2419-24.
39. Nturanabo F, Masu L, Kirabira JB. Novel applications of aluminium metal matrix composites, aluminium alloys and composites. In: Cooke KO, editor. Aluminium alloys and composites. London: IntechOpen; 2019 [cited 2021 Oct 18]. Available from: https://www.intechopen.com/chapters/67052.
40. Orbulov IN. Metal matrix syntactic foams produced by pressure infiltration-the effect of infiltration parameters. Mater Sci Eng A. 2013;583:11-9.
41. Gladysz GM, Chawla KK, Boccaccini AR. Preface: syntactic and composite foams special section. J Mater Sci. 2012;47(15):5625-6.
42. Szlancsik A, Katona B, Májlinger K, Orbulov IN. Compressive behavior and microstructural characteristics of iron hollow sphere filled aluminum matrix syntactic foams. Materials. 2015;8(11):7926-37.
43. Sazegaran H, Kiani-Rashid A, Khaki JV. Effects of sphere size on the microstructure and mechanical properties of ductile iron–steel hollow sphere syntactic foams. Int J Miner Metall Mater. 2016;23:676-82.
44. Rabiei A, Vendra L, Reese N, Young N, Neville BP. Processing and characterization of a new composite metal foam. Mater Trans. 2006;47(9):2148-53.
45. Rabiei A, Vendra LJ. A comparison of composite metal foam's properties and other comparable metal foams. Mater Lett. 2009;63:533-6.
46. Frage N, Levin L, Frumin N, Gelbstein M, Dariel MP. Manufacturing B_4C–(Al,Si) composite materials by metal alloy infiltration. J Mater Process Technol. 2003;143–144:486-90.
47. Dwivedi SP. Microstructure and mechanical behaviour of Al/B_4C metal matrix composite. Mater Today. 2020;25(4):751-4.
48. Ibrahim MF, Ammar HR, Samuel AM, Soliman MS, Songmene V, Samuel FH. Why Al-B_4C Metal Matrix composites? a review. In: Kitagawa J, editor. Advances in high-entropy alloys - materials research, exotic properties and applications. London: IntechOpen; 2021.
49. An Q, Cong X, Shen P, Jiang Q. Roles of alloying elements in wetting of SiC by Al. J Alloys Compd. 2019;784:1212-20.
50. Li X, Yan H, Wang Z, Li N, Liu J, Nie Q. Effect of heat treatment on the microstructure and mechanical properties of

a composite made of Al-Si-Cu-Mg aluminum alloy reinforced with SiC particles. Metals. 2019;9(11):1205.

51. Lekatou A, Karantzalis AE, Evangelou A, Gousia V, Kaptay G, Gácsi Z, et al. Aluminium reinforced by WC and TiC nanoparticles (ex-situ) and aluminide particles (in-situ): microstructure, wear and corrosion behaviour. Mater Des. 2015;65:1121-35.
52. Kumar PNS, Sachit TS, Mohan N, AkshayPrasad M. Dry sliding wear behaviour of Al –5Si-3Cu-0.5Mn alloy and its WC reinforced composites at elevated temperatures. Mater Today. 2021;44(1):566-72.
53. El-Mahallawi IS, Shash AY, Amer AE. Nanoreinforced cast Al-Si alloys with Al_2O_3, TiO_2 and ZrO_2 nanoparticles. Metals. 2015;5:802-21.
54. Hernandez-Sandoval J, Samuel AM, Samuel FH, Valtierra S. Effect of additions of SiC and Al_2O_3 particulates on the microstructure and tensile properties of Al–Si–Cu–Mg cast alloys. Int J Met Cast. 2016;10(3):253-63.
55. Oliveira PHF, Galvis JC, Martins JP, Carvalho ALM. Application of friction surfacing to the production of aluminum coatings reinforced with Al_2O_3 particles. Mater Res. 2017;20(2):603-20.
56. Xue J, Wu W, Ma J, Huang H, Zhao Z. Study on the effect of CeO_2 for fabricating in-situ TiB_2/A356 composites with improved mechanical properties. Mater Sci Eng A. 2020;786:139416.
57. Calin R, Pul M, Pehlivanli ZO. The effect of reinforcement volume ratio on porosity and thermal conductivity in Al-MgO composites. Mater Res. 2012;15(6):1057-63.
58. Karthikeyan G, Elatharasan G, Thulasi S, Vijayalakshmi P. Tensile, compressive and heat transfer analysis of ZrO_2 reinforced aluminum LM6 alloy metal matrix composites. Mater Today. 2021;37(2):303-9.
59. Rakshath S, Suresha B, Kumar RS, Saravanan I. Dry sliding and abrasive wear behaviour of Al-7075 reinforced with alumina and boron nitride particulates. Mater Today. 2020;22(3):619-26.
60. Lotfy A, Pozdniakov AV, Zolotorevskiy VS, El-khair MTA, Daoud A, Mochugovskiy AG. Novel preparation of Al-5%Cu/BN and Si_3N_4 composites with analyzing microstructure, thermal and mechanical properties. Mater Charact. 2018;136:144-51.
61. Fernández H, Ordoñez S, Pesenti H, González RE, Leoni M. Microstructure homogeneity of milled aluminum A356–Si_3N_4 metal matrix composite powders. J Mater Res Technol. 2019;8(3):2969-77.
62. He CN, Zhao NQ, Shi CS, Song SZ. Fabrication of aluminum carbide nanowires by a nano-template reaction. Carbon. 2010;48(4):931-8.
63. Laha T, Kuchibhatla S, Seal S, Li W, Agarwal A. Interfacial phenomena in thermally sprayed multiwalled carbon nanotube reinforced aluminum nanocomposite. Acta Mater. 2007;55(3):1059-66.
64. Noguchi T, Magario A, Fukazawa S, Shimizu S, Beppu J, Seki M. Carbon nanotube/aluminium composites with uniform dispersion. Mater Trans. 2004;45(2):602-4.
65. Mansoor M, Shahid M. Carbon nanotube-reinforced aluminum composite produced by induction melting. J Appl Res Technol. 2016;14(4):215-24.
66. Saravanan MSS, Babu SPK, Sivaprasad K. Mechanically alloyed carbon nanotubes (CNT) reinforced nanocrystalline AA 4032: synthesis and characterization. J Miner Mater Charact Eng. 2010;9(11):1027-35.
67. Bakshi SR, Keshri AK, Singh V, Seal S, Agarwal A. Interface in carbon nanotube reinforced aluminum silicon composites: thermodynamic analysis and experimental verification. J Alloys Compd. 2009;481(1-2):207-13.
68. Ferguson JB, Santa Maria JA, Schultz BF, Al–Al Rohatgi PK. $_2O_3$ syntactic foams—part II: predicting mechanical properties of metal matrix syntactic foams reinforced with ceramic spheres. Mater Sci Eng A. 2013;582:423-32.
69. Pan L, Rao D, Yang Y, Qiu J, Sun J, Gupta N, et al. Gravity casting of aluminum-Al_2O_3 hollow sphere syntactic foams for improved compressive properties. J Porous Mater. 2020;27:1127-37.
70. Su M, Wang H, Hao H, Fiedler T. Compressive properties of expanded glass and alumina hollow spheres hybrid reinforced aluminum matrix syntactic foams. J Alloys Compd. 2020;821:153233.
71. Gupta N, Pradeep KR. Metal Matrix syntactic foams: processing, microstructure, properties and applications. Lancaster: Destech Publications; 2015.
72. Luong DD, Strbik OM, Hammond VH, Gupta N, Cho K. Development of high performance lightweight aluminum alloy/SiC hollow sphere syntactic foams and compressive characterization at quasi-static and high strain rates. J Alloys Compd. 2013;550:412-22.
73. Fukunaga H. Aluminium metal matrix composites by reactive and semi-solid squeeze casting. In: Cantor B, Dunne F, Stone I, editors. Metal and ceramic Matrix composites. series in materials science and engineering. an oxford–kobe materials text. Bristol: Institute of Physics Publishing; 2004.
74. Lee JC, Lee J, Lee H. Methodologies to observe and characterize interfacial reaction products in (Al_2O_3)pAl and SiCppAl composites-using SEM, XRD, TEM. Scr Mater. 1996;35(6):721-6.
75. Geng J, Li Y, Xiao H, Li H, Sun H, Chen D, et al. Study fatigue crack initiation in TiB_2/Al-Cu-Mg composite by in-situ SEM and X-ray microtomography. Int J Fatigue. 2021;142:105976.
76. Bertrand R, Caty O, Mazars V, Denneulin S, Weisbecker P, Pailhes J, et al. In-situ tensile tests under SEM and X-ray computed micro-tomography aimed at studying a self-healing matrix composite submitted to different thermomechanical cycles. J Eur Ceram Soc. 2017;37(10):3471-4.
77. Selamat MS, Watson LM, Baker TN. XRD and XPS studies on surface MMC layer of SiC reinforced Ti–6Al–4V alloy. J Mater Process Technol. 2003;142(3):725-37.
78. Pai BC, Ramani G, Pillai RM, Satyanarayana KG. Role of Magnesium in cast aluminum alloy matrix composites. J Mater Sci. 1995;30:1903-11.
79. Rajan TPD, Pillai RM, Pai BC. Reinforcement coatings and interfaces in aluminium metal matrix composites. J Mater Sci. 1998;33:3491-503.
80. Geng L, Zhang H, Li H, Guan L, Huang L. Effects of Mg content on microstructure and mechanical properties of SiCp/Al-Mg composites fabricated by semi-solid stirring technique. Trans Nonferrous Met Soc China. 2010;20:1851-5.
81. Khalili V, Heidarzadeh A, Moslemi S, Fathyunes L. Production of Al6061 matrix composites with ZrO_2 ceramic reinforcement using a low-cost stir casting technique: microstructure, mechanical properties, and electrochemical behavior. J Mater Res Technol. 2020;9(6):15072-86.
82. Anas NS, Dash RK, Rao TN, Vijay R. Effect of carbon nanotubes as reinforcement on the mechanical properties of aluminum-copper-magnesium alloy. J Mater Eng Perform. 2017;26:3376-86.
83. Sanaty-Zadeh A. Comparison between current models for the strength of particulate-reinforced metal matrix nanocomposites with emphasis on consideration of Hall-Petch effect. Mater Sci Eng A. 2012;531:112-8.
84. Kim CS, Sohn I, Nezafati M, Ferguson JB, Schultz BF, Bajestani-Gohari Z, et al. Prediction models for the yield strength of particle-reinforced unimodal pure magnesium (Mg) metal matrix nanocomposites (MMNCs). J Mater Sci. 2013;48(12):4191-204.
85. Amirkhanlou S, Ji S, Zhang Y, Watson D, Fan Z. High modulus AlSiMgCu/Mg_2SiTiB_2 hybrid nanocomposite: microstructural characteristics and micromechanics-based analysis. J Alloys Compd. 2017;694:313-24.
86. Jiang L, Yang H, Yee JK, Mo X, Topping T, Lavernia EJ, et al. Toughening of aluminum matrix nanocomposites via spatial

arrays of boron carbide spherical nanoparticles. Acta Mater. 2016;103:128-40.

87. Cayron C. TEM study of interfacial reactions and precipitation mechanisms in Al2O3 short fiber or high volume fraction SiC particle reinforced Al-4Cu-1 Mg-0.5Ag squeeze-cast composites [thesis]. Lausanne: Swiss Federal Institute of Technology Lausanne (EPFL); 2001.
88. Lafabrier A, Fahs A, Louarn G, Aragon E, Chailan JF. Experimental evidence of the interface/interphase formation between powder coating and composite material. Prog Org Coat. 2014;77(7):1137-44.
89. Wang J, Duan HL, Zhang Z, Huang ZP. An anti-interpenetration model and connections between interphase and interface models in particle-reinforced composites. Int J Mech Sci. 2005;47(4–5):701-18.
90. Wang HW, Zhou HW, Peng RD, Mishnaevsky L Jr. Nanoreinforced polymer composites: 3D FEM modeling with effective interface concept. Compos Sci Technol. 2011;71(7):980-8.
91. Feest EA. Interfacial phenomena in metal-matrix composites. Composites. 1994;25(2):75-86.
92. Guo X. Processing of titanium–silicon carbide fibre composites. In: Cantor B, Dunne F, Stone I, editors. Metal and ceramic Matrix composites. series in materials science and engineering. an oxford–kobe materials text. Bristol: Institute of Physics Publishing; 2004.
93. Kaczmar JW, Naplocha K, Morgiel J. Microstructure and strength of Al2O3 and carbon fiber reinforced 2024 aluminum alloy composites. J of Materi Eng and Perform. 2014;23:2801-8.
94. Baik KH, Lee GC, Ahn S. Interface and tensile behavior of squeeze cast AC8A- Al_2O_3 composite. Scr Metall Mater. 1994;30:235-9.
95. Kandpal BC, Kumar J, Singh H. Fabrication and characterisation of Al_2O_3 /aluminium alloy 6061 composites fabricated by stir casting. Mater Today. 2017;4(2):2783-92.
96. Bradbury CR, Gomon JK, Kollo L, Kwon H, Leparoux M. Hardness of multi wall carbon nanotubes reinforced aluminium matrix composites. J Alloys Compd. 2014;585:362-7.
97. Tekmen C, Cocen U. The effect of Si and Mg on age hardening behavior of Al–SiCp composites. J Compos Mater. 2003;37(20):1791-800.
98. Maria JAS, Schultz BF, Ferguson JB, Rohatgi PK. Al–Al2O3 syntactic foams – part I: effect of matrix strength and hollow sphere size on the quasi-static properties of Al-A206/ Al_2O_3 syntactic foams. Mater Sci Eng A. 2013;582:415-22.
99. Sritharan T, Xia K, Heathcock J, Mihelich J. Matrix/reinforcement development for aluminium-based composites. In: Bhagat RB, Clauer AH, Kumar P, Ritter AM, editors. Metal and ceramic matrix composites: processing, modelling and mechanical behaviour, edited. Warrendale: TMS; 1990. p. 13-22.
100. Chawla KK. Composite materials: science and engineering. New York: Springer-Verlag; 1987. p. 83.
101. Pai BC, Ray S, Prabhakar KV, Rohatgi PK. Fabrication of Aluminium-Alumina (Magnesia) particulate composites in foundries using magnesium additions to the melts. Mater Sci Eng. 1976;24:31-44.
102. Zulfia A, Ramdaniawati D, Dhaneswara D. The role of Al_2O_3 nanoparticles addition on characteristic of Al6061 composite produced by stir casting process. Mater Sci Eng. 2018;6(2):39-47.
103. Schultz BF, Ferguson JB, Rohatgi PK. Microstructure and hardness of Al_2O_3 nanoparticle reinforced Al–Mg composites fabricated by reactive wetting and stir mixing. Mater Sci Eng A. 2011;530:87-97.
104. Chen Y, Liu X, Zhang T, Xie H, Zhao N, Shi C, et al. Interface intrinsic strengthening mechanism on the tensile properties of Al_2O_3/Al composites. Comput Mater Sci. 2019;169:2019.
105. Janowski GM, Pletka BJ. The influence of interfacial structure on the mechanical properties of liquid-phase-sintered aluminum-ceramic composites. Mater Sci Eng A. 1990;129:65-76.
106. Munitz A, Metzger M, Mehrabian R. The interface phase in Al−Mg/ Al_2O_3 composites. Metall Mater Trans, A Phys Metall Mater Sci. 1979;10(10):1491-7.
107. Hallstedt B, Liu ZK, Ågren J. Fibre-matrix interactions during fabrication of Al_2O_3 -Mg metal matrix composites. Mater Sci Eng A. 1990;129(1):135-45.
108. Xie B, Wang X. Thermo-physical properties and reaction process of SiCp/Al-7Si-5Mg Aluminum Matrix composites fabricated by pressureless infiltration. Rare Met Mater Eng. 2015;44(5):1057-61.
109. Henriksen BR, Gionnes I. Microstructure characterisation and mechanical properties of two SiC reinforced composites. In: Vincenzini P, editor. Advanced structural inorganic composites. Amsterdam: Elsevier Science Publishers; 1991, pp. 251-58.
110. Lucas IP, Yang NYC, Stephens II. Interface and near-interface microstructure of discontinuous reinforced metal matrix composites. In: MRS Proceedings; Pittsburgh; Proceedings. Cambridge: Cambridge University Press; 1992, p. 877-83.
111. Salvo L, L'Esperance G, Suery M, Legoux JG. Interfacial reactions and age hardening in A1-Mg-Si metal matrix composites reinforced with SiC particles. Mater Sci Eng A. 1994;177:173-83.
112. Kang HG, Kida M, Miyahara H, Ogi K. Age hardening behaviour of alumina continuous fibre reinforced Al-Si-Cu and Al-Si-Cu-Mg alloys. Int J Cast Met Res. 2002;15(1):1-7.
113. Sreekumar VM, Pillai RM, Pai BC, Chakraborty M. A study on the thermodynamics of In-situ $MgAl_2O_4$/Al MMC formation using amorphous silica sources. J Mater Process Technol. 2007;192-193:588-94.
114. Yang B, Sun M, Gan G, Xu C, Huang Z, Zhang H, et al. In situ Al_2O_3 particle-reinforced Al and Cu matrix composites synthesized by displacement reactions. J Alloys Compd. 2010;494(1-2):261-5.
115. Rohatgi PK, Asthana R, Das S. Solidification, structures, and properties of cast metal-ceramic particle composites. International Metals Reviews. 1986;31(1):115-39.
116. Bacciarini C, Mathier V. Aluminium AA6061 matrix composite reinforced with spherical alumina particles produced by infiltration: perspective on aerospace applications. J Metall. 2014;248542:1-10.
117. Mavrič A, Valant M, Cui C, Wang ZM. Advanced applications of amorphous alumina: from nano to bulk. J Non-Cryst Solids. 2019;521:119493.
118. Tavakoli AH, Maram PS, Widgeon SJ, Rufner J, Benthem K, Ushakov S, et al. Amorphous alumina nanoparticles: structure, surface energy, and thermodynamic phase stability. J Phys Chem C. 2013;117(33):17123-30.
119. Molins R, Bartout JD, Bienvenu Y. Microstructural and analytical characterization of $A1_2O_3$-(Al-Mg) composite interfaces. Mater Sci Eng A. 1991;135:111-7.
120. Ikeno S, Matsui H, Matsuda K, Uetani Y. Precipitation sequence of A12O3/Al-Cu-Mg and Al-Mg-Si composite materials. Mater Sci Forum. 2000;331-337:1193-8.
121. Matsuda K, Matsuki T, Uetani Y, Ikeno S. TEM observation of interface in A12O3particle dispersed Al-Mg-Si alloy composite materials. Mater Sci Forum. 2002;396-402:959-64.
122. Li J, Wang L, Zhong X, Xia M, Haigh SJ, Schumacher P. Cu segregation on the interface between $A1_2O_3$ substrate and Al-1.4Cu alloy. Mater Charact. 2017;129:300-4.
123. Liu G, Zhang Z, Shang JK. Interfacial microstructure and fracture of $A1_2O_3$ particulate reinforced Al-Cu composite. Acta Metall Mater. 1994;42(1):271-82.
124. Abdel-Azim AN, Shash Y, Mostafa SF, Younan A. Casting of 2024-A1 alloy reinforced with $A1_2O_3$ particles. J Mater Process Technol. 1995;55(3-4):199-205.

125. Naveen E, Ramanan N, Arvind R, Dinesh I, Mayandi A, Naveen D. Analysis of mechanical and wear properties of Al-SiO_2 composite material. J Innov Mech Eng. 2018;1(1):1-5.
126. Pattnaya A, Madhu N, Panda AS, Sahoo MK, Mohanta K. A comparative study on mechanical properties of Al-SiO_2 composites fabricated using rice husk silica in crystalline and amorphous form as reinforcement. Mater Today. 2018;5(2):8184-92.
127. Nallusamy S, Logeshwaran J. Effect on aluminium metal matrix composite reinforced with nano sized silica particles. J Metastable Nanocryst Mater. 2017;29:25-34.
128. Schwabe U, Wolff LR, Loo FJJ, Ziegler G. Corrosion of technical ceramics by molten aluminium. J Eur Ceram Soc. 1992;9:407-15.
129. Zhu H, Dong K, Huang J, Li J, Wang G, Xie Z. Reaction mechanism and mechanical properties of an aluminum-based composite fabricated in-situ from Al–SiO_2 system. Mater Chem Phys. 2014;145(3):334-41.
130. Gregolin E, Goldenstein H, Gonçalves MC, Santos RG. Aluminium matrix composites reinforced with Co-continuous interlaced phases aluminium-alumina needles. Mater Res. 2002;5(3):337-42.
131. Orbulov IN, Nemeth A, Dobranszk J. XRD and EDS investigations of metal matrix composites and syntactic foams. In: 13th European Conference on X-Ray Spectrometry; 2008 Jun 16-20; Cavtat. Paris: Société Chimique de France; 2008.
132. Wang D, Shi Z. Aluminothermic reduction of silica for the synthesis of alumina-aluminum-silicon composite. J Mater Synth Process. 2001;9(5):241-6.
133. Li B, Luo B, He K, Zeng L, Fan W, Bai Z. Effect of aging on interface characteristics of Al–Mg–Si/SiC composites. J Alloys Compd. 2015;649:495-9.
134. Lee JC, Lee HI, Ahn JP, Shi ZL, Kim Y. Modification of the interface in SiC/Al composites. Metall Mater Trans, A Phys Metall Mater Sci. 2000;31:2361-8.
135. Asthana R. Reinforced cast metals: part II evolution of the interface. J Mater Sci. 1998;33:1959-80.
136. Dudek HJ, Kleine A, Borath R, Neite G. Interfaces in alumina-fibre-reinforced aluminium piston alloys. Mater Sci Eng A. 1993;167(1-2):129-37.
137. Mahmoud TS, El-Kady EY, Al-Shihiri ASM. Corrosion behaviour of Al/SiC and Al/Al_2O_3 nanocomposites. Mater Res. 2012;15(6):903-10.
138. Wang S, Dudek HJ. Fibre-matrix interaction in the δ- Al_2O_3-fibre reinforced aluminium piston alloy. Mater Sci Eng A. 1996;205(1-2):180.
139. Lee JC, Kirn GH, Lee J, Lee HI. Interfacial reactions in the squeeze-cast (SAFFIL+C)/SAE 329 Al composite. Metall Mater Trans, A Phys Metall Mater Sci. 1997;28:1251-9.
140. Sato A, Mehrabian R. Aluminum matrix composites: fabrication and properties. Metall Mater Trans, B, Process Metall Mater Proc Sci. 1976;7:443-51.
141. Kim Y, Lee JC. Processing and interfacial bonding strength of 2014Al matrix composites reinforced with oxidized SiC particles. Mater Sci Eng A. 2006;420(1-2):8-12.
142. Moghadam AD, Ferguson JB, Schultz BF, Rohatgi PK. In-situ reactions in hybrid aluminum alloy composites during incorporating silica sand in aluminum alloy melts. AIMS Materials Science. 2016;3(3):954-64.
143. Nourouzi S, Damavandi E, Rabiee SM. Microstructural and mechanical properties of Al- Al_2O_3 composites focus on experimental techniques. Int J Microstruct Mater Prop. 2016;11(5):383-98.
144. Moghadam AD, Omrani E, Menezes PL, Rohatgi PK. Effect of in-situ processing parameters on the mechanical and tribological properties of self-lubricating hybrid aluminum nanocomposites. Tribol Lett. 2016;62(25):1-10.
145. Venugopal S, Karikalan L. Microstructure and physical properties of hybrid metal matrix composites AA6061-TiO_2-SiC via stir casting techniques. Mater Today. 2021;37(2):1289-94.
146. Kumar GBV, Gouda PSS, Pramod R, Rao CSP. Synthesis and characterization of TiO_2 reinforced Al6061 composites. Adv Compos Lett. 2017;26(1):18-23.
147. Ramkumar KR, Natarajan S. Tensile properties and strengthening effects of Al 3003 alloy weldment reinforced with TiO_2 nanoparticles. Compos, Part B Eng. 2019;175:107159.
148. Chaudhury SK, Panigrahi SC. Role of processing parameters on microstructural evolution of spray formed Al–2Mg alloy and Al–2Mg–TiO_2 composite. J Mater Process Technol. 2007;182(1-3):343-51.
149. Saboori A, Chen X, Badini C, Fino P, Pavese M. Reactive spontaneous infiltration of Al-activated TiO_2 by molten aluminum. Trans Nonferrous Met Soc China. 2019;29(3):657-66.
150. Maity PC, Chakraborty PN, Panigrahi SC. Processing and properties of Al/Al_2O_3 (TiO_2) in situ particle composite. J Mater Process Technol. 1995;53(3-4):857-70.
151. Feng CF, Froyen L. Formation of Al_3Ti and Al_2O_3 from an Al–TiO_2 system for preparing in-situ aluminium matrix composites. Compos, Part A Appl Sci Manuf. 2000;31(4):385-90.
152. Dake LS, Lad RJ. Electronic and chemical interactions at aluminum/TiO_2 (110) interfaces. Surf Sci. 1993;289(3):297-306.
153. Shin JH, Choi HJ, Bae DH. Evolution of the interfacial layer and its effect on mechanical properties in TiO_2 nanoparticle reinforced aluminum matrix composites. Mater Sci Eng A. 2013;578:80-9.
154. Chao ZL, Zhang LC, Jiang LT, Qiao J, Xu ZG, Chi HT, et al. Design, microstructure and high temperature properties of in-situ Al_3Ti and nano-Al_2O_3 reinforced 2024Al matrix composites from Al-TiO_2 system. J Alloys Compd. 2019;775:290-7.
155. Ghanaraja S, Ramanuja CM, Gangadhara GCJ, Abhinandhan KS. Fabrication and mechanical properties of Al (Mg)-TiO_2 based in-situ composites. Mater Today. 2015;2(4-5):1282-90.
156. Khodabakhshi F, Simchi A, Kokabi AH, Švec P, Simančík F, Gerlich AP. Effects of nanometric inclusions on the microstructural characteristics and strengthening of a friction-stir processed aluminum–magnesium alloy. Mater Sci Eng A. 2015;642:215-29.
157. Sabooni S, Karimzadeh F, Abbasi MH. A study on the mechanochemical behavior of TiO_2–Al–Si system to produce Ti_5Si_3–Al_2O_3 nanocomposite. Adv Powder Technol. 2012;23(2):199-204.
158. Roy D, Chakravarty D, Mitra R, Manna I. Effect of sintering on microstructure and mechanical properties of nano-TiO_2 dispersed Al65Cu20Ti15 amorphous/nanocrystalline matrix composite. J Alloys Compd. 2008;460(1-2):320-5.
159. Muñoz MC, Gallego S, Beltrán JI, Cerdá J. Adhesion at metal–ZrO_2 interfaces. Surf Sci Rep. 2006;61(7):303-44.
160. Zhu H, Ai Y, Min J, Wu Q, Wang H. Dry sliding wear behavior of Al-based composites fabricated by exothermic dispersion reaction in an Al–ZrO_2–C system. Wear. 2010;268(11):1465.
161. Moya JS, Steier HP, Requena J. Interfacial reactions in aluminum alloys/mullite–zirconia composites. Compos, Part A Appl Sci Manuf. 1999;30(4):439-44.
162. Rostami RB, Tajall M. Improvements in microstructure and mechanical properties of Al–Si–Cu alloy–Al_2O_3 nanocomposite modified by ZrO_2. J Mater Res. 2014;29(21):2505-13.
163. Baghchesara MA, Abdizadeh H, Baharvandi HR. Microstructure and mechanical properties of aluminum alloy matrix composite reinforced with ZrO_2 particles. Asian J Chem. 2010;22(5):3824-34.
164. Cho YH, Lee HC, Im YR, Kwon SW. The effect of alloying elements on the microstructure and mechanical properties of Al-12Si cast alloys. Mater Sci Forum. 2003;426:339.
165. Sharma A, Roh MH, Jung D, Jung JP. Effect of ZrO2 Nanoparticles on the microstructure of Al-Si-Cu filler for low-temperature Al

brazing applications. Metall Mater Trans, A Phys Metall Mater Sci. 2016;47:510-21.

166. Daoud A, Abou-Elkhair MT, Rohatgi P. Wear and friction behavior of near eutectic Al–Si+ZrO_2 or WC Particle Composites. Compos Sci Technol. 2004;64(7-8):1029-40.

167. Liu H, Han L, Zhao C, Li Y. Interfacial research on interpenetrating network structure ZrO_2/Al-Mg composites prepared by Extrusion Freeform Fabrication 3DP and pressureless infiltration. Mater Lett. 2020;275:128068.

168. Guo RF, Lv HC, Shen P, Hu ZJ, Jiang QC. Lamellar-interpenetrated Al−Si−Mg/Al_2O_3−ZrO_2 composites prepared by freeze casting and pressureless infiltration. Ceram Int. 2017;43(3):3292-7.

169. Gao T, Cui XL, Li XY, Li H, Liu XF. Morphological evolutions and growth patterns of Zr-containing phases in aluminum alloys. CrystEngComm. 2014;16:3548-57.

170. Barzilai S, Aizenshtein M, Froumin N, Frage N. Interface phenomena in the Y_2O_3/(Al–Cu) system. Mater Sci Eng A. 2006;420(1-2):291-5.

171. Barzilai S, Aizenshtein M, Shapiro-Tsoref E, Froumin N, Frage N. Interface interaction and wetting in the Y_2O_3/(Al–Cu–Y) system. Int J Adhes Adhes. 2007;27(5):358-61.

172. Matsubara I, Paranthaman M, Allison SW, Cates MR, Beshears DL, Holcomb DE. Preparation of Cr-doped Y3Al5O12 phosphors by heterogeneous precipitation methods and their luminescent properties. Mater Res Bull. 2000;35(2):217-224.

173. Yu Z, Wu G, Jiang L, Sun D. Effect of coating Al_2O_3 reinforcing particles on the interface and mechanical properties of 6061 alloy aluminium matrix composites. Mater Lett. 2000;59:2281-4.

174. Kim GH, Hong SM, Lee MK, Kim SH, Ioka I, Kim BS, et al. Effect of oxide dispersion on dendritic grain growth characteristics of cast aluminum alloy. Mater Trans. 2010;51(10):1951-7.

175. Zhang T, Li DY. Improvement in the resistance of aluminum with yttria particles to sliding wear in air and in a corrosive medium. Wear. 2001;251:1250-6.

176. Moussa ME, El-Hadad S, Khalifa W. Influence of chemical modification by Y_2O_3 on eutectic Si characteristics and tensile properties of A356 alloy. Trans Nonferrous Met Soc China. 2019;29:1365-74.

177. Bouaeshi WB, Li DY. Effects of Y_2O_3 addition on microstructure, mechanical properties, electrochemical behavior, and resistance to corrosive wear of aluminum. Tribol Int. 2007;40(2):188-99.

178. Oliveira M, Agathopoulos S, Ferreira JMF. The influence of Y_2O_3-containing sintering additives on the oxidation of Si3N4-based ceramics and the interfacial interactions with liquid Al-alloys. J Eur Ceram Soc. 2005;25(1):19-28.

179. Anaee RAM. Thermodynamic and kinetic study for corrosion of Al-Si-Cu/Y_2O_3 composites. Asian J Chem. 2014;26(14):4469-74.

180. Ponappa K, Aravindan S, Rao PV. Influence of Y_2O_3 particles on mechanical properties of magnesium and magnesium alloy (AZ91D). J Compos Mater. 2012;47(10):1231-9.

181. Divakar R, Rozario JG, Savithri V. Fabrication and testing of aluminum metal matrix composites with Graphene and Yttrium oxide. Int J Adv Res. 2016;4(2):1226-31.

182. Amra M, Ranjbar K, Hosseini SA. Microstructure and wear performance of Al5083/CeO_2/SiC mono and hybrid surface composites fabricated by friction stir processing. Trans Nonferrous Met Soc China. 2018;28(5):866-78.

183. Hassannejad H, Moghaddasi M, Saebnoori E, Baboukani AR. Microstructure, deposition mechanism and corrosion behavior of nanostructured cerium oxide conversion coating modified with chitosan on AA2024 aluminum alloy. J Alloys Compd. 2017;725:968-75.

184. Skrzekut T, Kula A, Sugamata M. Structural characterization of mechanically alloyed AlMg-CeO_2 composite. Key Eng Mater. 2015;641:10-6.

185. Skrzekut T, Kula A, Blaz L, Wloch G, Sugamata M. High-strength and thermally stable Al-CeO_2 composite produced by means of mechanical alloying. Int J Mater Res. 2014;105(3):1-6.

186. Balaji P, Arun R, JegathPriyan D, Ram IM, Manikandan E. Comparative study of Al 6061 alloy with Al 6061– Magnesium Oxide (MgO) composite. Int J Sci Eng Res. 2015;6(4):408-12.

187. Kheder ARI, Marahleh GS, Al-Jamea DMK. Strengthening of aluminum by SiC, Al_2O_3 and MgO. Jordan J Mech Ind Eng. 2011;5(6):533-41.

188. Fujii H, Nakae H. Equilibrium contact angle in the magnesium oxide/aluminium system. Acta Mater. 1996;44(9):3567-73.

189. Mohammed G, El-Gamal S. The role of MgO nanoparticles addition, and γ-irradiation on the microstructural, and tensile properties of Al-1100 alloy. J Compos Mater. 2021;55(16):2135-49.

190. Yar AA, Montazerian M, Abdizadeh H, Baharvandi HR. Microstructure and mechanical properties of aluminum alloy matrix composite reinforced with nano-particle MgO. J Alloys Compd. 2009;484(1-2):400-4.

191. Lin Y, Zhang Q, Liu T, Wang H, Lu J, Ye Y, et al. Sol-gel MgO coating on glass microspheres for inhibiting excessive interfacial reaction in Al-Mg matrix syntactic foam. J Alloys Compd. 2019;798:59-66.

192. Calin R, Citak R. Effect of Mg content in matrix on infiltration height in producing MgO/Al composite by vacuum infiltration method. MSF. 2007;546–549:611-4.

193. Sun Y, Li Y, Li H, Yan M, Tong S, Sun J. Formation mechanism of dense anti-oxidation layer in Al-Si-MgO composites sintered in air condition. Ceram Int. 2018;44(4):3987-92.

194. Sun J, Wang D, Zhang Y, Sheng C, Dargusch M, Wang G, et al. Heterogeneous nucleation of pure Al on MgO single crystal substrate accompanied by a $MgAl_2O_4$ buffer layer. J Alloys Compd. 2018;753:543-50.